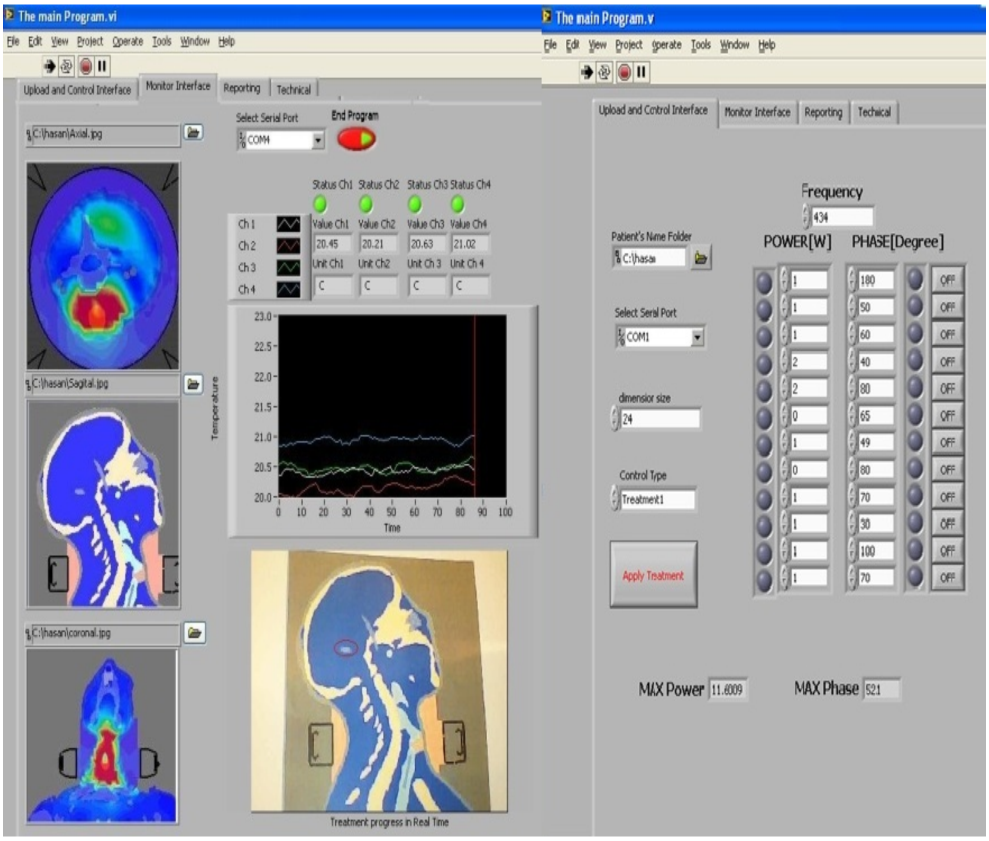

Towards Quality Assured Hyperthermia Treatment Delivery

Master's Thesis in Biomedical Engineering

HASAN MASUD

Biomedical Electromagnetics Group
Department of Signals & Systems
Chalmers University of Technology
Gothenburg, Sweden.

Master's Thesis 2013
Report No: EX004/2013

Abstract

To ensure high quality treatment, the accuracy and the stability of any system has to be evaluated prior to clinical use. Another important factor of accurate treatment delivery is a graphical user interface (GUI) which secures against any possible misinterpretation while providing comprehensive information about the treatment. In this project, we worked on stability estimation and GUI development of hyperthermia system. For stability estimation, routine calibrations were performed and the channel performance was measured for a duration of one month. From the long time measurement we have found that the system performance is stable up to one month in both phase and power contrast. The best, worst and intermediate performing channels were identified for further analysis. By mean of a short time measurement on these three channels we have found the worst case error in the phase is 6% (14°, at frequency 434 MHz, allowed phase range -180° to $+52.5^{\circ}$) and the worst case error in the power is 12.5% (-1.25 W) at maximum allowed power which are not align with design criteria. Thus, restriction of the maximum power, avoiding long time system running are proposed to resolve the short time measurement errors and performing system calibration in one month interval is recommended. The GUI containing four tabs was developed in Labview. The four tabs are: Uploading Treatment Plan and Controlling the system, Visualizing of the temperature profile of different sensors and comparing real time treatment with the planned one, Documenting the treatment and the last one is for technical reference. The perfusion effects on biological tissue due to the blood perfusion were investigated in the last part of the project. It has been found that there are no changes in dielectric property of the biological tissue due to the perfusion.

Acknowledgements

At first, I would like to thank the Almighty who enabled me to complete my thesis work and the whole master program. I would like to thank my examiner Dr. Andreas Fhager for his hearty cooperation. I would earnestly take the opportunity to extend my gratitude to my supervisor Dr. Hana Dobsicek Trefna for giving me the chance to work on this wonderful project and for her never ending assistance during the entire work. I would also like to thank Dr. Johanna Gellermann for her motivation and suggestion in different phase of this work. Finally, I would like to give a special thanks to my mother, father and better-half for supporting me to stay thousand miles away from home though I know they miss me a lot.

Hasan Masud, Gothenburg, Sweden, 21/02/13.

Contents

List of Figures

1

Introduction

CAncer is one of the most dangerous death causing disease in the world. In a statistics presented by World Health Organization, it is known that, the number of death due to cancer is increasing all over the world and if it continues it will reach up to 16 million in 2020 [5]. Therefore, the world demands more precise and effective cancer treatment. When group of cells grow very fast and uncontrollably, those cells are called cancer cells. In traditional cancer treatment these cancer cells are damaged along with some normal cells; which causes side effects. Hyperthermia treatment is a medical procedure in which the temperature inside the tumor tissue is increased up to the therapeutic level without affecting surrounding normal tissues. Temperature above $42.6\,^{\circ}$ is cytotoxic to the tumors and tumors become more sensible to radiation or certain drugs[4]. Nowadays it is being used together with radiation therapy for certain types of cancer treatment.

Deep seated tumor treatment based on microwave regional hyperthermia uses an array of antennas to transfer heat to the desired region of the body or to the tumors. Usually a ring shape applicator is used. By controlling the power and phase of the channels the desired interference can be achieved in the tumor and it is also used for controlling heating.[3]

In Chalmers University of Technology, Biomedical Electromagnetics group have been developing clinical system for head and neck cancer treatment. The long term stability of the newly developed system has to be derived before going to the clinics [6]. The main purpose of this thesis project is to assure a quality treatment delivery to the patient and making the system user friendly. More specifically, to ensure quality treatment it is needed to analyze the whole system performance. That means we have to measure the stability of the amplifier system over time. Based on the result, an interval period for routine calibration is to be proposed. It is important to have a good steering and monitoring interface which would make operators to feel comfortable to work with and also prevent any mistakes in treatment delivery. The interface requires to be interactive and informative. The documentation of the treatment includes the treatment given to the patient and the results of the treatment. This documentation can be used for further assessment. So it is also important for a new system to have an automatic documentation option for the whole procedure. Another important factor is to investigate how does perfusion effects dielectric property of the biological tissue being exposed by microwave energy. It will also be investigated as a sub project.

This report organized in four main chapters. Chapter One includes the background and the motivation of the work. The Second chapter explains how the work progresses and how the work is done. Then it comes with chapter three which would explain the final results. The next chapter four includes the discussion and conclusions of the projects. It also contains a bibliography and an appendix at the end.

2

Preliminaries

Cancer is one of the most dangerous and death causing disease in the world. In the present world many different types of cancer treatment exists such as chemotherapy, surgery and radiotherapy. Hyperthermia can be used as an addition to increase the sensitivity of chemotherapy and radiotherapy [2]. The present chapter takes account of the general summary of hyperthermia technique which will cover basic principle, general types, sources of heat, superiority and basic system architecture.

2.1 Hyperthermia

It is technique of elevating tissue temperature and commonly used to treat cancer cells. It is reported that temperature above 42 ° are cytotoxic to the cancer cells. According to Cabuy E [7] , Hyperthermia is a cancer treatment in which tumor cells are exposed to elevated temperature ranges between 41 °-45 °C by applying EM energy for a specific amount of time for causing destruction to cancer cells. Temperatures exceeding above limits causes cytotoxic effect and termed as ablation.[7]

The Molecular and Cellular events in Hyperthermia treatment depends on treatment temperature. Different phenomena occurs in different therapeutic temperature which is shown in figure 2.1.

2.1.1 Hyperthermia Heating Techniques

There are several ways to achieve desired temperature in the tissues. In general three major techniques are used to do so; electromagnetic (EM) heating, Thermal Conduction and ultra sound. The thermal conduction technique is a simple one which delivers heat in the tumor through hot balloons and usually inserted into the body's natural cavity. The ultrasound technique allows a very good control on temperature distribution but in the bone interface there is danger of high acoustic absorption. As a result of this, patient could feel discomfort and pain due to heating of bone. Due to the demerits of Thermal conduction and Ultrasound, EM heating technique is prominent source of heating in Hyperthermia. The EM applicators can be two types based on how it delivers the heat into the tumor cells ; first one is external and second one

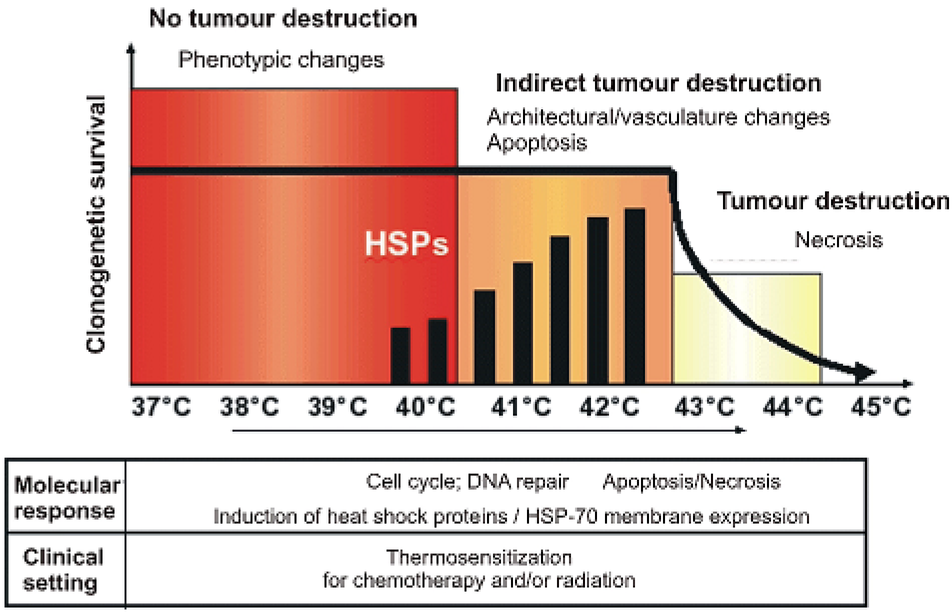

Figure 2.1: Molecular and Cellular events in Hyperthermia treatment. [adopted from [1]]

is interstitial. For giving treatment externally by using EM technique non-invasive applicator having antenna array is used; shown in figure 2.1. Now, if we consider the targeted area of treatment , Hyperthermia can be three types mainly- local, regional and whole body.[8]

In the following section we will have brief description about local and whole body hyperthermia and detail description about regional hyperthermia heating technique because the system retarding this project using this technique.

2.1.2 Local Hyperthermia

This technique is mostly used for treating superficial tumors. In recent days this technique is in highest clinical practice among other HT techniques in the treatment of superficial tumors.The operating frequency of EM energy used in this technique is normally 0.1-2.45 GHz and which allows the skin depth up to 3 cm [3]. The EM energy is imparted into the tumor by using an antenna applicator and a water bolus placed according to figure 2.2 .The water bolus is used for providing dielectric coupling interface between body and applicator. The EM energy generated by EM generator and directed towards the applicator. All these are controlled by a specially programmed and equipped computer. There is a feedback system for measuring temperature inside and around the tumor. This temperature can be measured by using invasive multi-sensor temperature probes such as fiber optic probes. [3]

2.1.3 Whole Body Hyperthermia

There are some special type of cancers namely carcinoma, for treating these type of cancers it is some times required to maintain a steady state temperature up to 42 ° C in the full body of the patient and the duration is around 1 hour. For treating this type

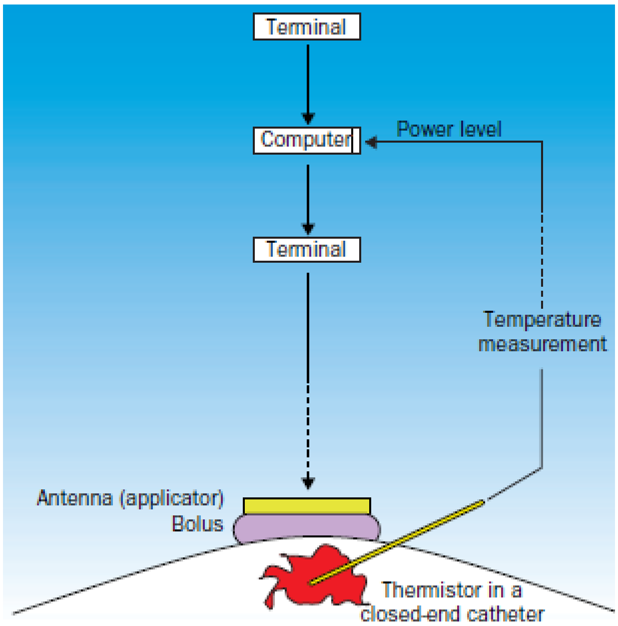

Figure 2.2: Principle of local Hyperthermia treatment. [adopted from [2]]

of patient with whole body approach nowadays microwave and infrared techniques are used in clinics.[3]

2.1.4 Regional Hyperthermia

This type of technique is used to treat tumor located in a deep region of the body. In this technique the EM energy is imparted in such a way that it becomes concentrated in the tumor and the temperature at the neighboring healthy tissue remains at a level below the critical one. In practice a circular antenna array is placed circumferentially around the targeted region of the patient. The focusing spot in the tumor site can be achieved by controlling the phase and magnitude of the energy radiated from the antenna feed points. The penetration depth of EM waves depends on the operating frequency of the waves. For head and neck region this operating frequency is 434 MHz [3]. A typical instrument used for regional hyperthermia is shown in figure 2.3

2.2 Chalmers Hyperthermia System

Figure 2.4 is the existing prototype of the microwave hyperthermia system of Chalmers. In order to bring this system into the clinics the stability of the system needs to be evaluated with an user friendly graphical interface (GUI). In figure 2.5 the block diagram of the present system is shown. The system has twelve channels. The oscillator generates a sinusoidal signal having power -0 dBm with frequency range 300-1000 MHz.The low power signal is pre-amplified by the help of a 26 dB power amplifier(MPA), the signal is divided into 12 channels using a microwave power divider. The MPA is beneficial for two reasons; firstly, it compensates the losses on the way from oscillator to the input power amplifiers (PA) and secondly, it helps to reduce the harmonic distortions by allowing low power output from the oscillator. In each channel the phase is adjusted

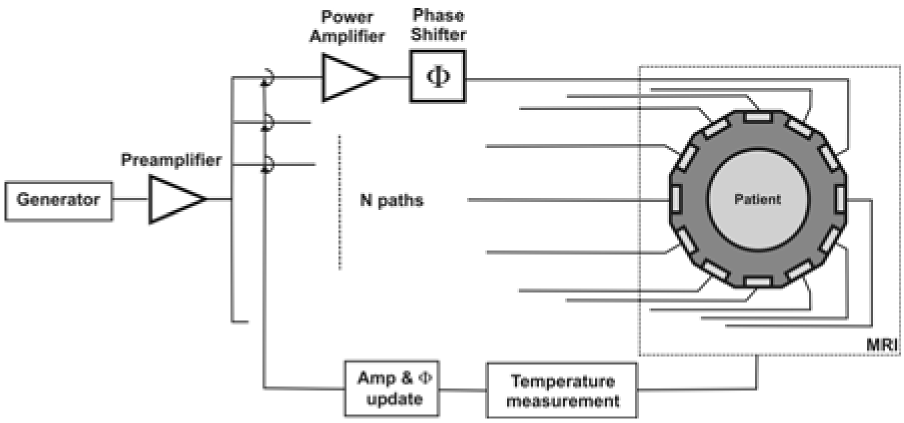

Figure 2.3: Block Diagram of regional hyperthermia treatment. reproduced from [3]

by an 8-bit digital phase shifter. The signal is then amplified by a voltage driven power amplifier. The output of the PA depends on the frequency. The output from the PA is then connected to the one of the 12 antennas through a bidirectional coupler. The arm in the forward direction is connected with a 12 channel switch and the other arm is connected to a detector which detects the reflected signal from the antenna; giving the impedance matching information. If the reflected back power is over 50% of the requested power then the system is switched off automatically.

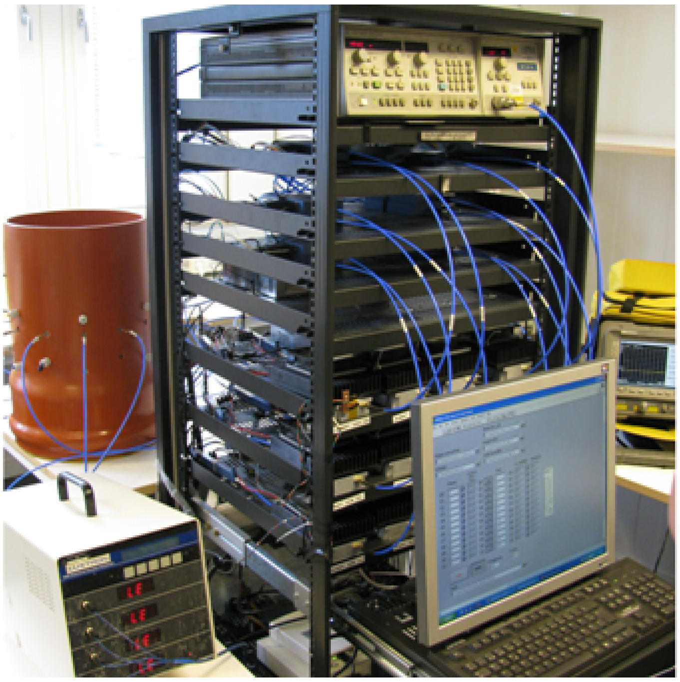

Figure 2.4: The exsisting hyperthermia prototype. reproduced from [4]

The whole electronic system is controlled by a computer through data acquisition modules (DAQs). The graphical user interface is developed in NI Labview v.8.5 with implemented matlab routine [4]. All the hardware used for controlling the applicator and the channels are connected through three data acquisition modules (DAQs). The first DAQ NI (USB - 6509) controls the phase shifters , second one (NI PCI- 6703) is

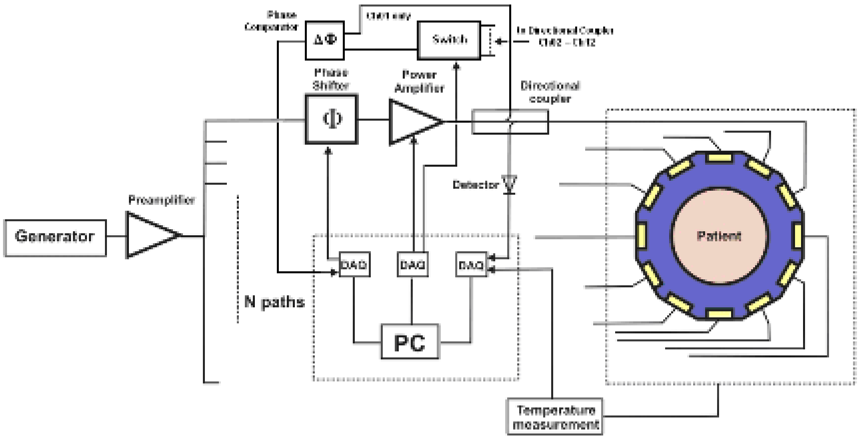

Figure 2.5: Block diagram of hyperthermia prototype.reproduced from [4]

used to control PA and the third one receives information from power detector and phase comparators.The whole system is steered by a user interface shown in figure 2.6.

The user interface is difficult to interpret for end user and demands more realistic.

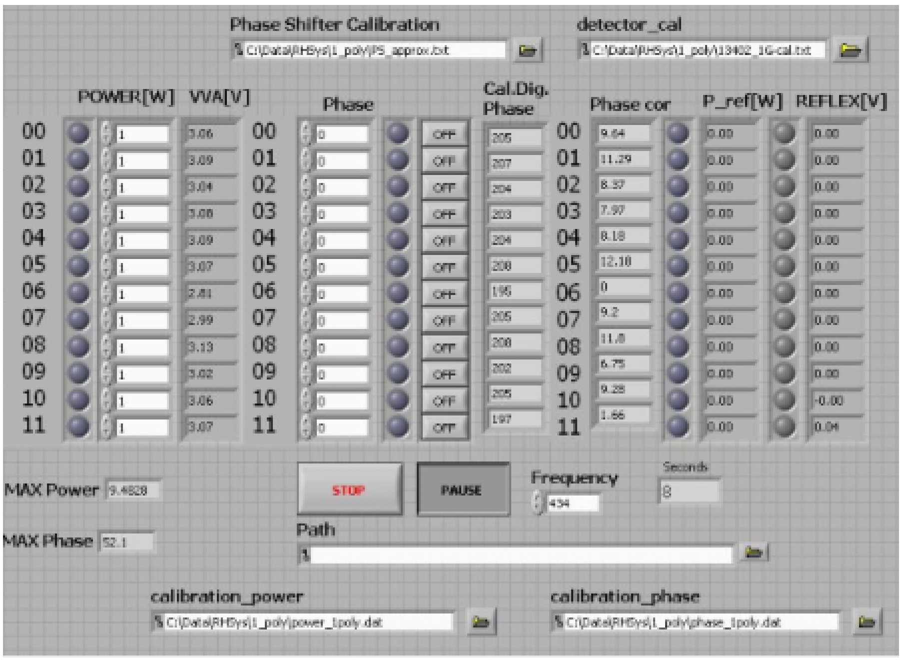

Figure 2.6: Old Graphical User Interface. reproduced from [4]

2.3 Purpose of the Thesis

2.3.1 Stability Measurement

To access the stability of the system the output power and phase accuracy were tested. It was observed that all the channels has similar power output profile. In the worst case the difference between the requested and measured power were ranging 6% . This results are shown in figure 2.8. The phase error in channel 3 was 4% in the frequency range of 300MHz to 1GHz, shown in figure 2.7. These measurements were done in an arbitrary time interval. The goal of this thesis is to perform stability measurements and evaluate the changes over time to define the schedule for calibration.

Bakker **at al** [9], found error in power accuracy 5% and phase accuracy 5 ° for their system. This level of accuracy allows maximum 1 mm focus position error in case of muscle tissue at 434 MHz. It is important for our system to achieve at least this level of accuracy to ensure high focusing precision.

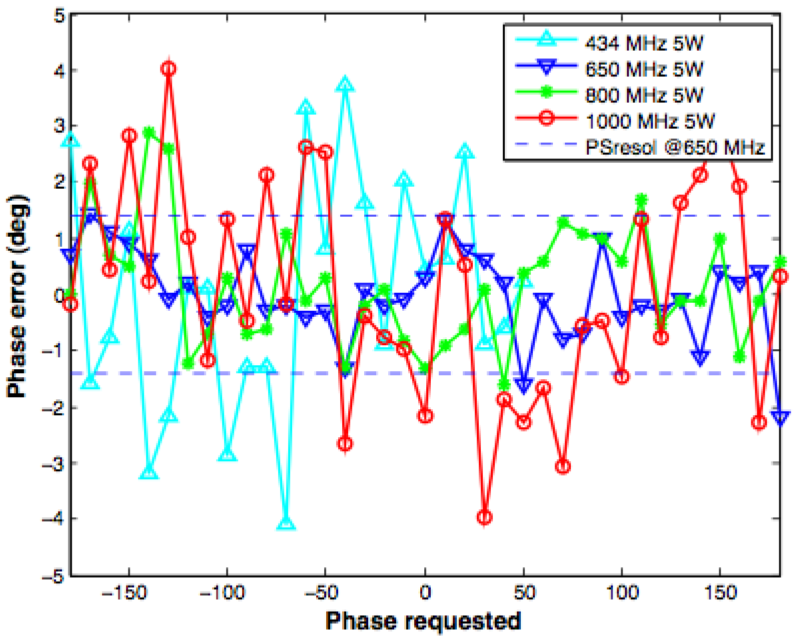

Figure 2.7: single channel output phase characteristics. reproduced from [4]

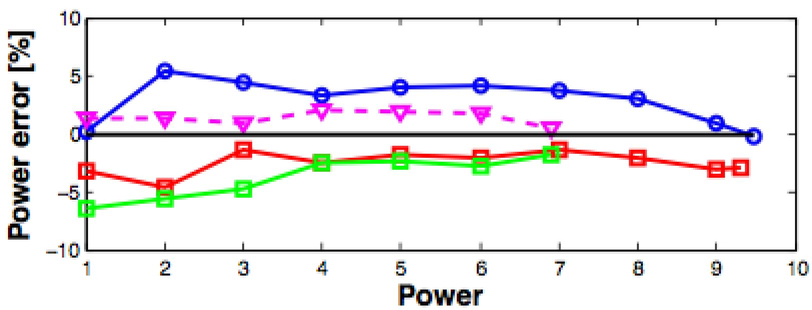

Figure 2.8: single channel output power characteristics. reproduced from [4]

2.3.2 The Graphical User Interface

The graphical user interface (GUI) of any system provides a comprehensive and interactive way to operate and control the system. The present interface was developed to be used by engineers in order to control the system. In this project, the goal is to develop a comprehensive and interactive graphical user interface (GUI) so that clinical personnels feel comfortable to work with the system. There will be options for using treatment plan. The temperature measurement with several sensors will be visualized in a form of graph. There will be chances to observe the comparison between the planned treatment and the treatment on progress. The temperature and other treatment information must be documented for further reporting or analysis.

2.3.3 Microwave and Perfusion

In microwave hyperthermia we use interference of microwave signals in the targeted tissue. When temperature increases in the tissue, perfusion also increases in the surrounding vessels. In this sub-project the effects of increased perfusion on the conductivity and Permittivity of the blood will be investigated.

3

Materials and Methods

In this chapter, the main focus is to describe how the project has been carried out, what were the equipments used, how we proceed though the work. It would be also discussed how the decision were made in different phases of the work.

3.1 Routine Calibration

In this section the detail setup of the calibration process and the connected equipments. Further analysis process are going to be described.

The microwave hyperthermia system able to operate in a wide range of frequency. Thus frequency dependent phenomena like power level fluctuations and nonlinear characteristics due to signal amplification, different phase delay in the channels, insertion losses can be expected. To resolve this problem a calibration of the system is required. This calibration need to be one in a regular basis and channel by channel.

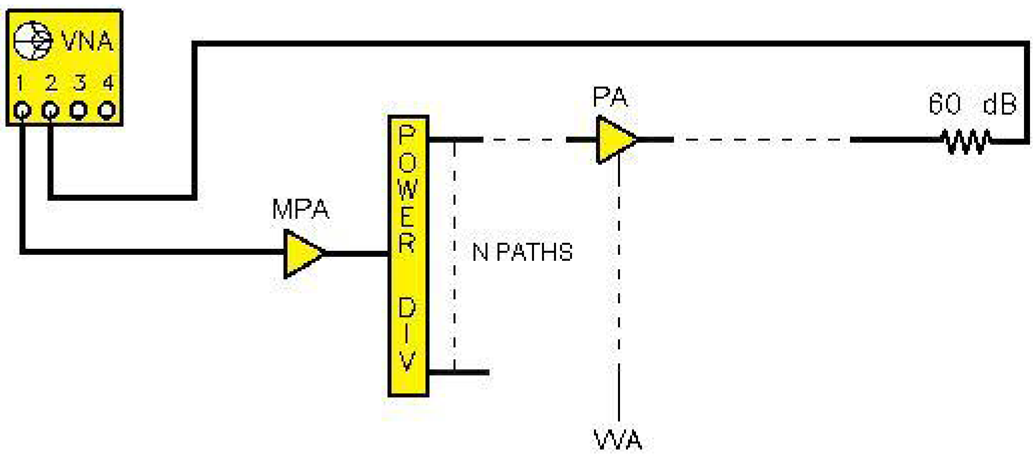

Figure 3.1: The setup diagram of the calibration process.

The calibration setup is shown in figure 3.1. The S21 parameter is measured by using a vector network analyzer (VNA) (E8362B,Agilent, USA) and the calibration is based on controlled changes of this parameter. As a input microwave source in place of oscillator the port 1 of the VNA was connected to the input side of the MPA. The settings in VNA used are 701 harmonics in the range of 300-1000MHz which provides 1 MHz frequency resolution in the calibration process. The input power from the VNA is 1 dBm.

The port 2 is connected to the output of each channel which was being calibrated. A 60 dB attenuator (Weinschel Associates) was placed in between the port 2 and output of the channel. In the Lab-view control interface, the desired channel switch is turned on and the driving voltage of PA is increased gradually in step 0.1 from 2.5 V to 5 V in the maximum level. The S21 measurement are done with an averaging factor of 10 for each step of increased power and saved in the calibration file. This procedure is repeated for all the 12 channels. Then using this S21 measurements and some approximation by polynomial functions the characteristics of output power and phase is determined.

The calibration files are then used to make system calibration files for amplifier phase and power changes. The system has been calibrated several times to observe the system performance in different time interval.

3.2 Stability Measurement

For phase and power measurement, the same setup as figure 3.1 is used. In this case only the measured phase or power at the marker level from the interface of the VNA are recorded.

To access the system performance phase of every channels were measured with requested phase ranges -180 to the maximum allowed phase. The phase measurement of every single channel was repeated for three different requested power level. The power measurements are performed for every channels starting from power 1 W by increasing with a step 1 W up-to the maximum allowed power. In the power measurement the phase requested is kept unchanged. All the measurement are recorded manually.

3.2.1 Long Term Measurement

The purpose of this measurement is to find who the system performance deteriorate with comparatively long intervals. For this measurement, the system is calibrated in one week and three measurements are performed in next three consecutive weeks. After three complete measurements all these three measurement results are plotted to justify the performance changes or not. We found the system is quite stable. The ideal channel , worst case channel and average channel are identified for further evaluation. These channels are ch00, ch05 and ch09. A new short time measurement is planned on these three channels and with five frequencies. In this long time measurement, we performed the measurements for all the 12 channels. The whole measurements at one frequency takes about ten to 12 hours. This why we choose one frequency (434 MHz) to reduce the complexity. Then. The channels are

3.2.2 Short Term Measurement

In this part it was intended to find out the system performance changes in very short period of time and with working load. The system performance are measured three times in one day intervals directly after the calibration are made. In this case only three channels identified in the long term measurements are measured. These measurements are however extended to five frequencies. These frequencies are 300 MHz, 434 MHz, 650 MHz, 800 MHz and 1 GHz.The whole measurement took about one week.

3.3 Interface Development

For sake of user satisfaction and error less treatment delivery the graphical interface needs to have more interactive element like graphs, images, video and noticeable buttons according to Fitts' Law [10]. In previous design (figure 2.5) temperature data acquisition was through DAQ modules which is not necessary in this case because we have only receiving data. Thus, labveiw code is developed for temperature data acquisition through USB ports.

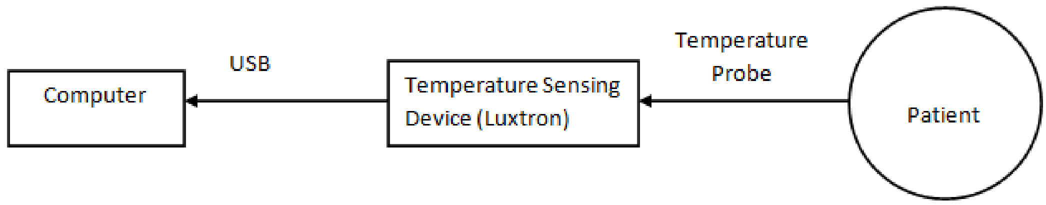

Figure 3.2: Model of lab-view coding for temperature measurement.

The combined temperature data from four sensors (luxtron) reach to the computer serially to the USB port of the computer illustrated in figure 3.2.These data are read into labview by VISA VI. Different tasks have been done to separate serial data into corresponding channel data. Finally channel wise temperature data are plotted in real time. To reduce programming complexity we include four sub-VI in temperature plotting section. The options for uploading planned SAR distribution for the treatment are creating by image readable VI and displayed in the front panel. Different programming structures are used to be able to select a treatment from a set of treatments. Vision Acquisition Express is used to facilitate the viewing of a real time video. For report generation we used different functions which performs different tasks.

3.4 Perfusion Effect

The frequency dependency of the dielectric property of the biological tissues has been studied for last few decades. The temperature dependence of dielectric properties of the biological tissues were also investigated [11].Hyperthermia increases temperature and thereby perfusion at the tumor site. However to our best knowledge the perfusion dependence of dielectric property have not been studied. Thus it is important to investigate the effects on the dielectric property of biologicals tissue due to the change in perfusion in the arteries.

The dielectric probe (85070E, Agilent) is used to measure the dielectric properties of the blood phantom inside the arteries and surrounded by muscle phantom. The dielectric probe is connected to the vector network analyzer (VNA) (E8362B, Agilent) through a flange free open-ended probe. The perfusion is maintained by a DC pump driven by 24 V DC supply. The temperature of both phantoms are maintained at the room temperature. Silicon based tiny tube are used as blood arteries. The muscle phantom is taken in a plastic jar and the arteries are immersed into it. The dielectric probe is placed on the arteries. The measurements are done in the frequency range of 0.2 - 3 GHz. The complete setup of dielectric property measurement is shown in figure 3.3

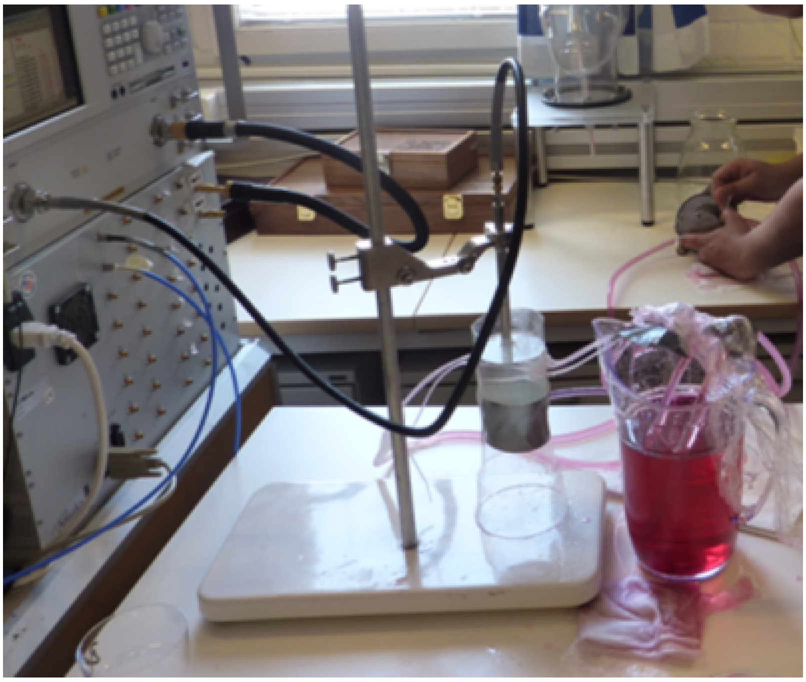

Figure 3.3: The setup of complete perfusion effect test.

Figure 3.4: Dielectric Probe in close contact to the blood vessel phantom.

3.4.1 Muscle and Blood Phantom Preparation

The muscle phantom is prepared by 40 % sugar and 0.4 % sodium chloride. Blood phantom is prepared with 0.12 % sodium chloride (salt) and a drop of pink tincture. The given percentages are total volume percentages. The mixtures were stirred up for a sufficient amount of time to ensure that all the ingredients are mixed properly in to solution.After the phantom preparation, blood phantom is injected into the blood arteries by using the pump and muscle phantom is poured into the plastic container.

3.4.2 Dielectric Property Measurements

At first the dielectric probe is calibrated. The dielectric properties of the phantoms are measured first.Then,the dielectric probe is placed in close contact to the arteries as visible from figure 3.4. The dielectric properties inside the arteries without any perfusion is measured and the measurement file is stored in the VNA. These two measurements are performed to see the difference of added silicon based tiny tube. The flow is then increased gradually and for every step the dielectric properties are recorded in VNA. The main idea was to identify weather there is any dielectric change or not when flow is changed. After the setup only the flow of blood phantom inside the artery were varied while keeping other parameter constant. Seven different flow rate are used in three different measurements. At every single step flow rate are increased and the dielectric property file is saved in VNA. These saved data files are analyzed to plot dielectric property of blood phantom.

4

Results

In this chapter, at first the short time system performance will be presented followed by the newly developed graphical user interface.Finally the perfusion effect results.
To present the results several comparison based plots are used. For the sake of readability and to present the results precisely, the most significant results are shown here. Rest of them will be included in appendix.

4.1 System Performance

In this section the amplifier stability over time is presented. Two type of investigations; one long time and one short time measurements are performed. The results from short time study are presented mostly since it represents the final conclusion.

Figure 4.1 and 4.2 shows the result of **channel 00** from three different measurements performed in three different dates with one day intervals and three different requested power level at frequency 434 MHz and 1GHz respectively. The highest error in phase at 1 and 5 W are $10\,^{\circ}$, at maximum power is close to $9\,^{\circ}$ for frequency 434 MHz . The lowest phase error at all power levels are $0\,^{\circ}$ for frequency 434 MHz. For frequency 1GHz, the highest error in phase at all the power levels are in between $7\,^{\circ}$ to $8\,^{\circ}$. The lowest error in this case are between $-2\,^{\circ}$ to $-2.5\,^{\circ}$.

Similarly,Figure 4.3 and 4.4 shows the result of **channel 05** from three different measurements performed in three different dates with one day intervals and three different requested power level at frequency 434 MHz and 1GHz respectively. The highest error in phase at power level 1 W is $11\,^{\circ}$, at power level 5 W is $14\,^{\circ}$ and for maximum allowed power level is $11\,^{\circ}$ for frequency 434 MHz . The lowest phase error at all power levels are between $1\,^{\circ}$ to $2\,^{\circ}$ for frequency 434 MHz. For frequency 1GHz, the highest error in phase at all the power levels are in between $6\,^{\circ}$ to $8.5\,^{\circ}$. The lowest error in this case are between $0\,^{\circ}$ to $-2.5\,^{\circ}$.

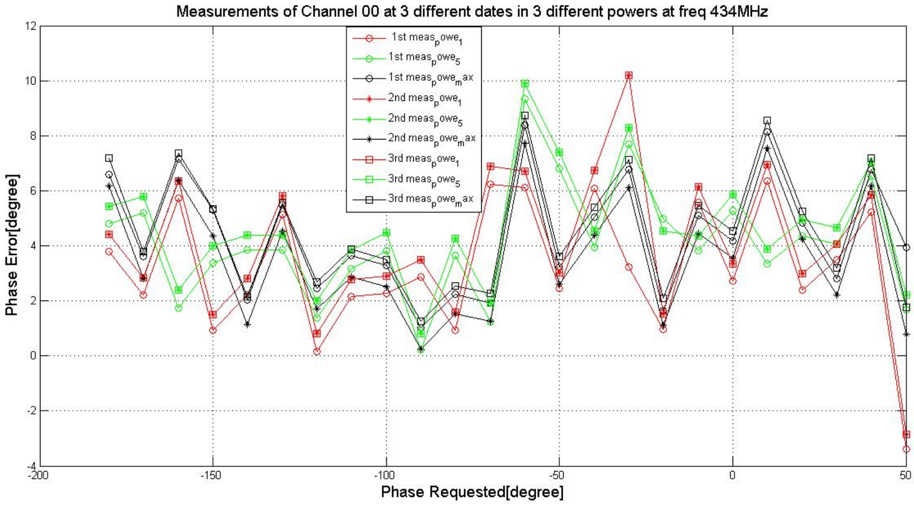

Figure 4.1: Phase measurements of channel 00 done in three different dates and three different requested power level in a single frequency 434 MHz.

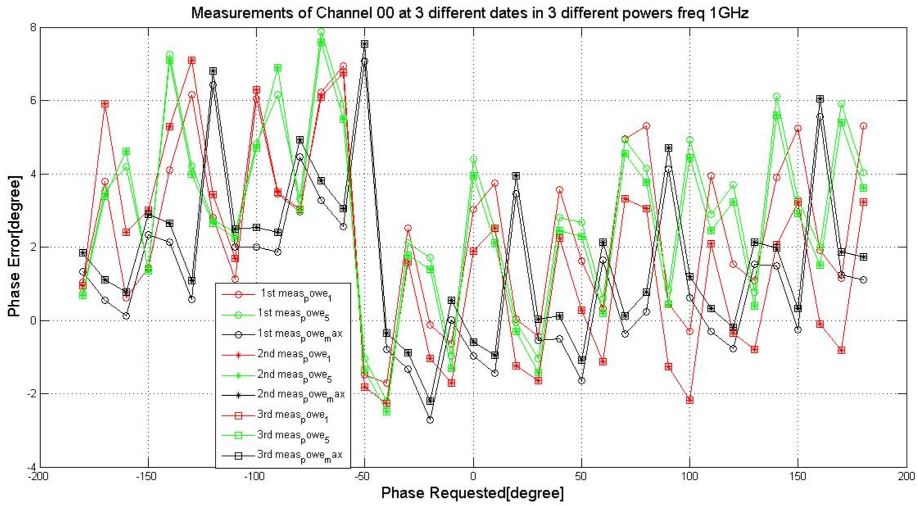

Figure 4.2: Phase measurements of channel 00 done in three different dates and three different requested power level in a single frequency 1GHz.

Figure 4.5 shows the result of **channel 09** from similar measurements at frequency 300 MHz. Figure 4.6 shows the comparison with of phase response at maximum power level (9.8229 W) with power requested 9.5 W. The yellow line in figure 4.6 indicates the respective response at 9.5 W. If the maximum power response after requested phase -110° is not considered, the highest and lowest error in phase at all three power levels are between $+5^\circ$ to -6°.

Figure 4.7 shows the result of **channel 09** from similar measurements at frequency 434 MHz. The highest phase error at all the power levels are between 6° to 8.5° and the lowest error in phase at all three power levels are between 0° to 1°.

Figure 4.8,4.9, 4.10 shows power response of three channels **ch00 , ch05 and ch09** respectively. The results of these plots are based on power measurements of

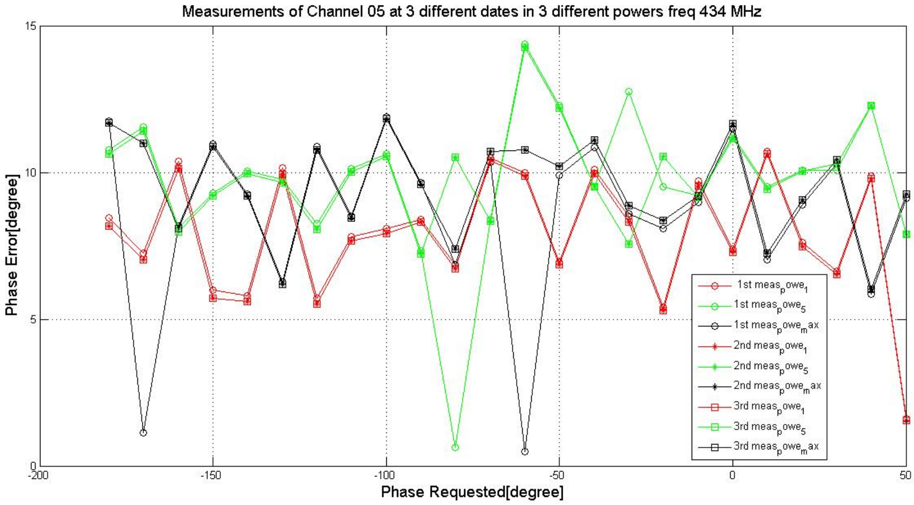

Figure 4.3: Phase measurements channel 05 done in three different dates and three different requested power level in a single frequency 434 MHz.

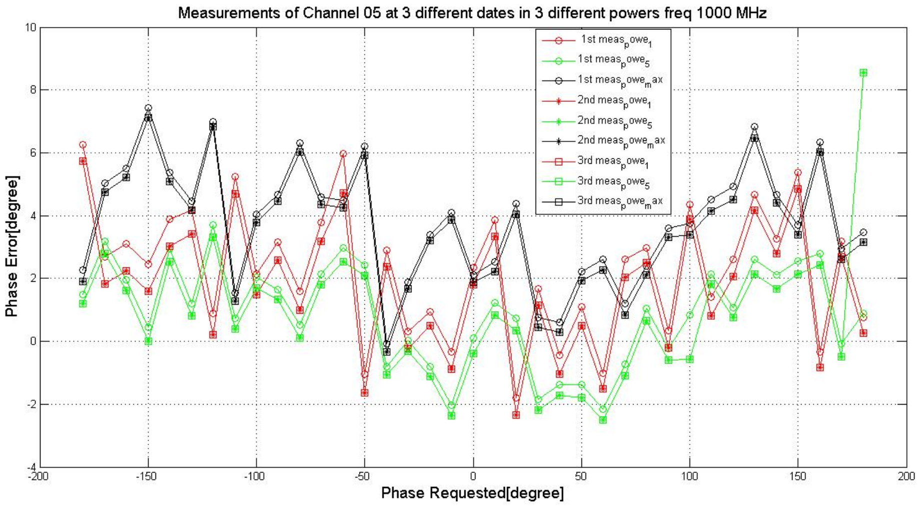

Figure 4.4: Phase measurements channel 05 done in three different dates and three different requested power level in a single frequency 1GHz.

three different dates in five different frequencies. In figure 4.8 power error at 300 MHz is in between +0.25 W to -0.25W, at 434 MHz is in between +0.65 W to -0.55 W, at 650 MHz is in between +0.6 W to -0.55 , at 800 MHz is in between 0 W to -0.5 W and at 1 GHz is in between +0.3 W to -0.55 W.

In figure 4.9 power error at 300 MHz is in between 0 W to -0.5 W, at 434 MHz is in between +0.65 W to -0.25 W, at 650 MHz is in between -0.25 W to -1.25 W , at 800 MHz is in between 0 W to -0.9 W and at 1 GHz is in between +0.1 W to -01.25 W.

In figure 4.10 power error at 300 MHz is in between +0.4 W to -0.6 W, at 434 MHz is in between +0.25 W to -0.25 W, at 650 MHz is in between +0.25 W to -0.6 W , at 800 MHz is in between 0.4 W to -0.4 W and at 1 GHz is in between +0.4 W to -0.4 W.

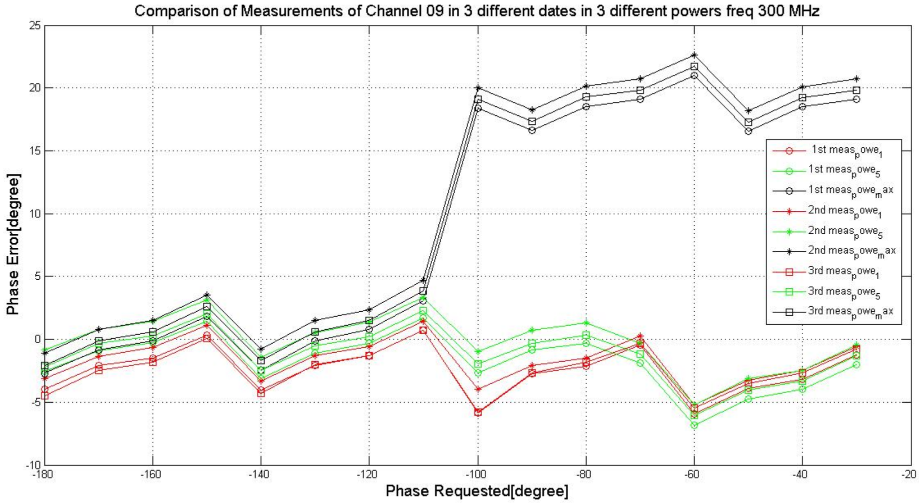

Figure 4.5: Phase measurements channel 09 done in three different dates and three different requested power level in a single frequency 300 MHz.

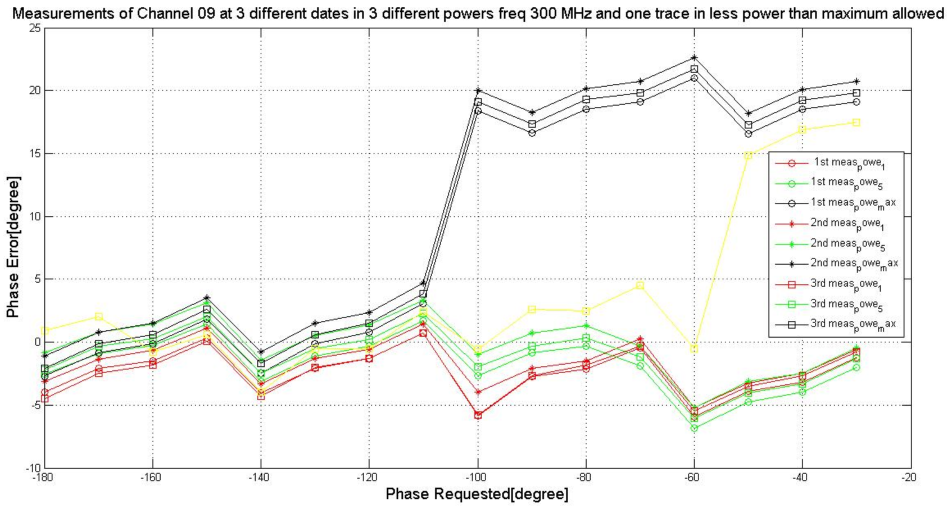

Figure 4.6: A unique Phase measurements channel 09 done in three different dates and maximum requested power level in a single frequency 300 MHz.

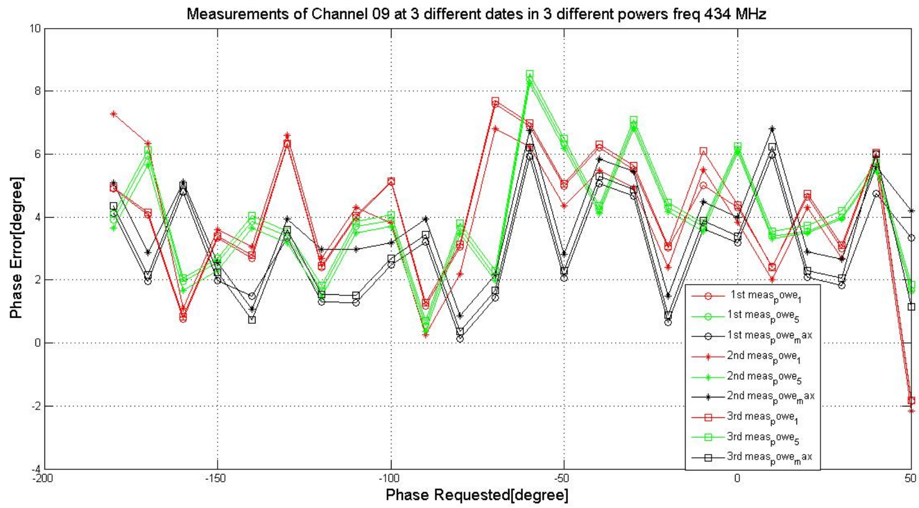

Figure 4.7: Phase measurements channel 09 done in three different dates and three different requested power level in a single frequency 434 MHz.

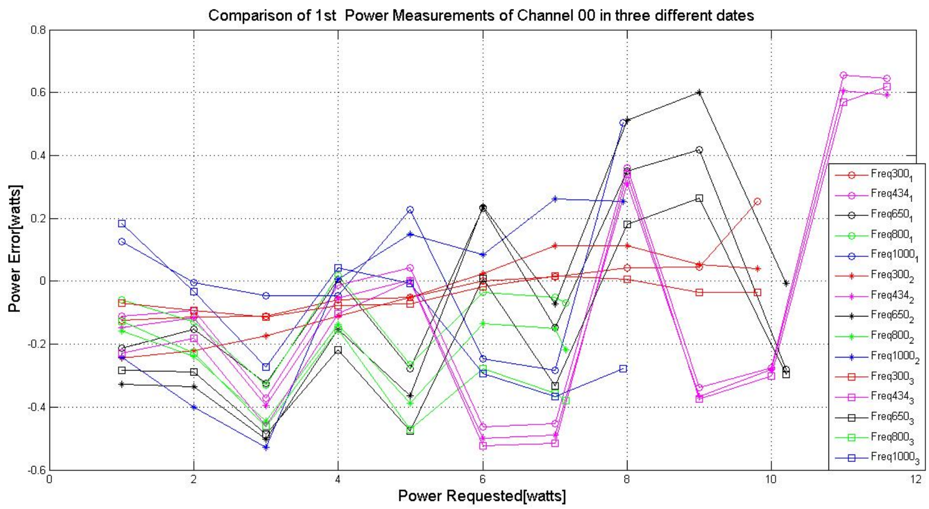

Figure 4.8: Power measurements of channel 00 done in three different dates and five different frequencies.

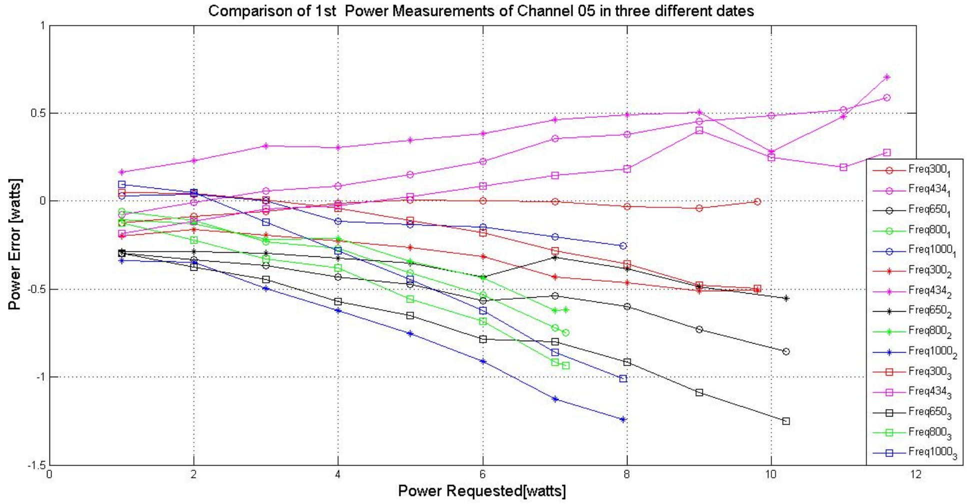

Figure 4.9: Power measurements of channel 05 done in three different dates and five different frequencies.

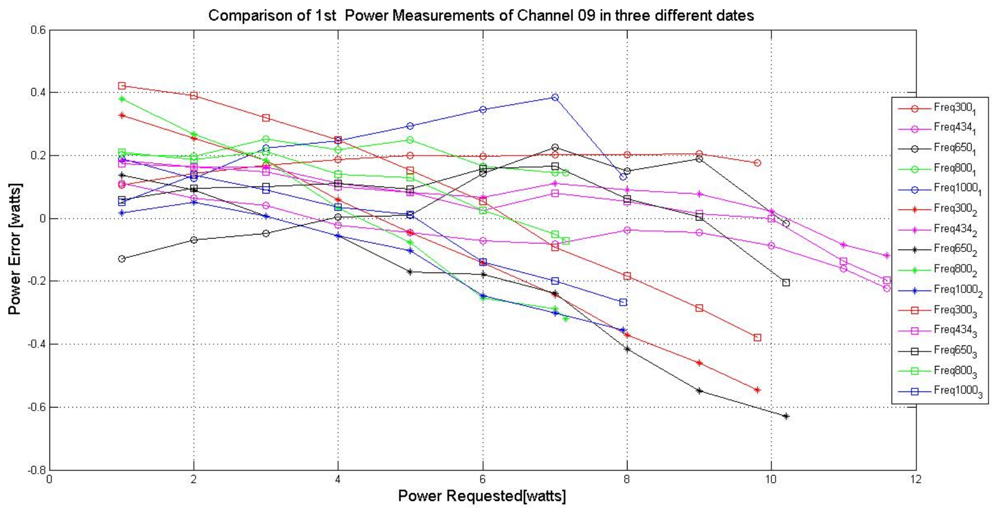

Figure 4.10: Power measurements of channel 09 done in three different dates and five different frequencies.

The figure 4.11 is the power stability results from the long time measurements for **ch04** to **ch05**. The red lines shows three measurements in three weeks of **ch04** and the green lines shows three measurements in three weeks of **ch05**. The phase error in both channels lies between $+6^\circ$ to -6° . In the worst case the phase error is 14° which means 6% in case of third measurement of **ch00** at maximum power shown in figure A.3 . Thus, in long time the system shows high stability in phase.

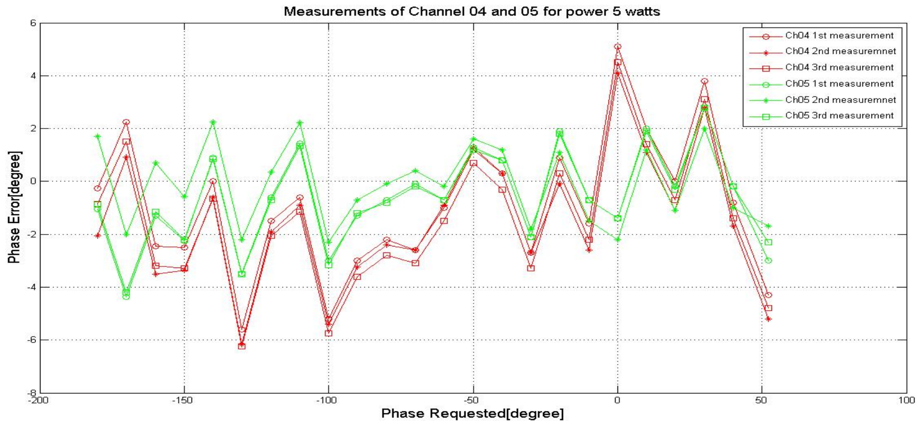

Figure 4.11: long time Phase measurements of channel 04 and channel 05 at 5 watts

The figures 4.12, 4.13, 4.14 are the power stability results from the long time measurements for **ch00** to **ch11**. The power error in all the cases lies between +0.5 W to -0.55 W which gives 5.5% error except for ch 01. Thus, in long time the system shows high stability in power as well.

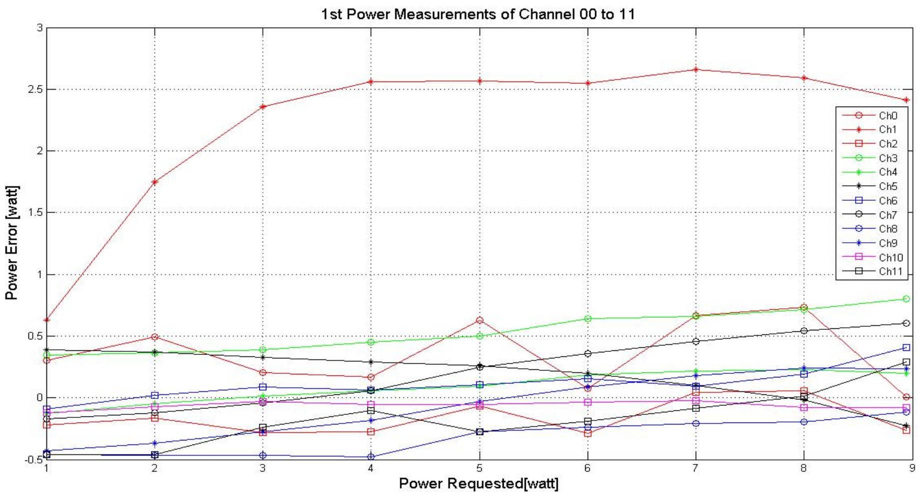

Figure 4.12: 2nd Long time power stability measurements for ch 00 to ch11

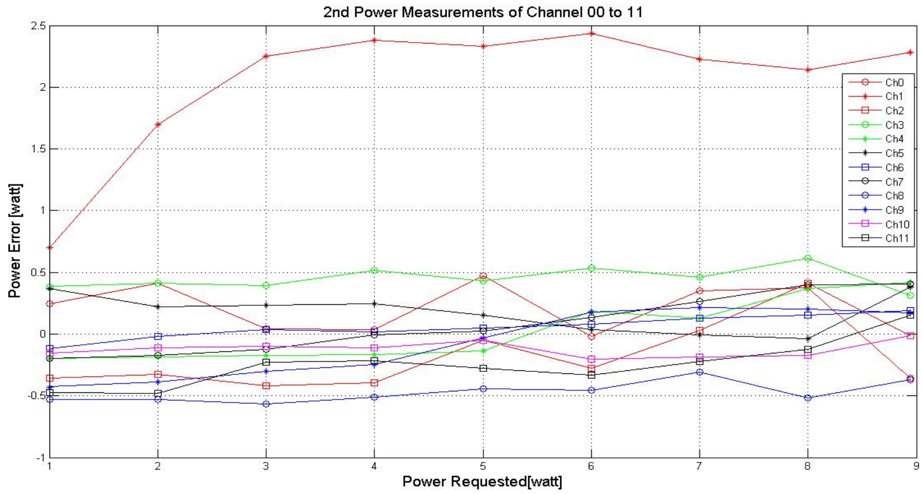

Figure 4.13: 2nd Long time power stability measurements for ch 00 to ch11

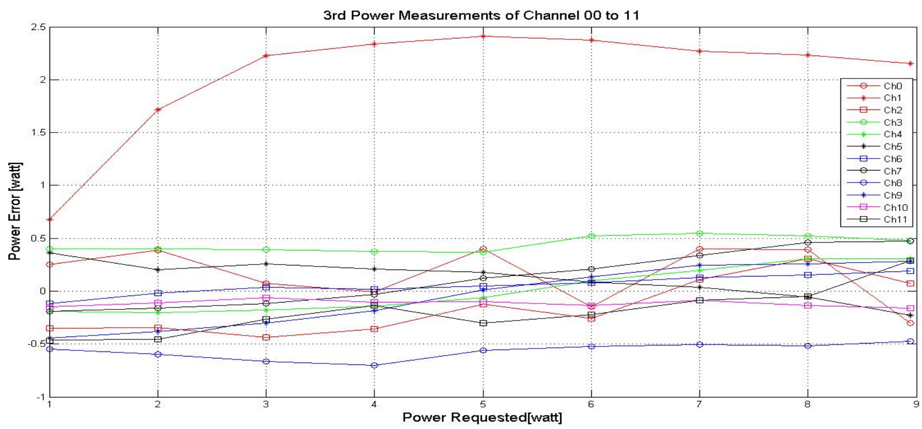

Figure 4.14: 3rd Long time power stability measurements for ch 00 to ch11

4.2 The New User Interface

The new interface is a integration of four tab based interface performing four different type of tasks; first one is uploading all the information and control, second one is for monitoring the treatment procedure, the third one is for reporting the treatment and the final one is for technical use.

The uploading and control interface in figure 4.15, provides the possibility to select the treatment from a set of four treatments and visualize the corresponding SAR images first and then applying it to the patient. Without confirmation of the operator the treatment would not be applied to the system as we use an apply treatment button to ensure correct treatment delivery. After changing the treatment corresponding values of phase and power of the antennas will be displayed on the array indicators. It has the option to change the treatment manually as well. We use power and phase control in the same interface to ensure the real treatment image to the operator. While using manual control this array indicator will change to control element that means we can change the value from here directly. However, in either case the operator has to press the apply button to confirm that he wants to use this treatment. The other indicators are moved to the technical interface to make this interface readable and usable because those indicators might me confusing to the clinical personnel.

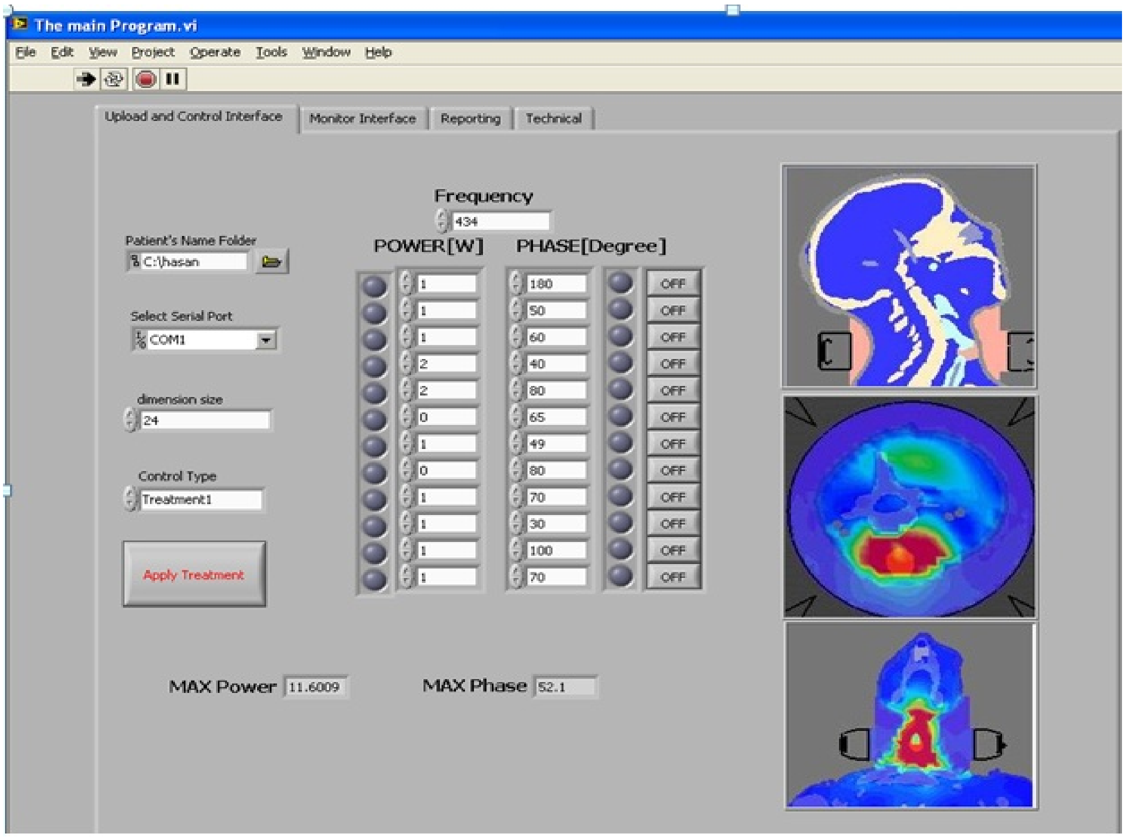

Figure 4.15: The New Uploading and Control Interface

The monitoring interface in figure 4.16 contains options of displaying SAR images, temperature profiles of sensors (Time-Temperature) and a real time video. The SAR image will help to compare the treatment delivery. We use same images in both interface because once the operators are done with uploading then he/she would like to continue with monitoring interface to follow the treatment. In this case having a feedback of applied treatment will help him to monitor the treatment development and identify quickly if anything goes wrong. The time-temperature graph indicates the heat development inside the tumor which one can be used to observe the temperature in a desired position is increased or maintained as expected or not. The informations form this graph can be used later on to find out mean , highest and lowest temperature. Thus temperature data will be logged in a file for further analysis. The real time video can be used to monitor the patient movement. Audio based feedback is also possible with the video to notify the operator if the patient has any discomfort or complain. This option can also be used for comparing real SAR images to the planned SAR images from three views; Axial, Coronal and Sagital. We need a imaging system for this purpose which can provide SAR information slice by slice.

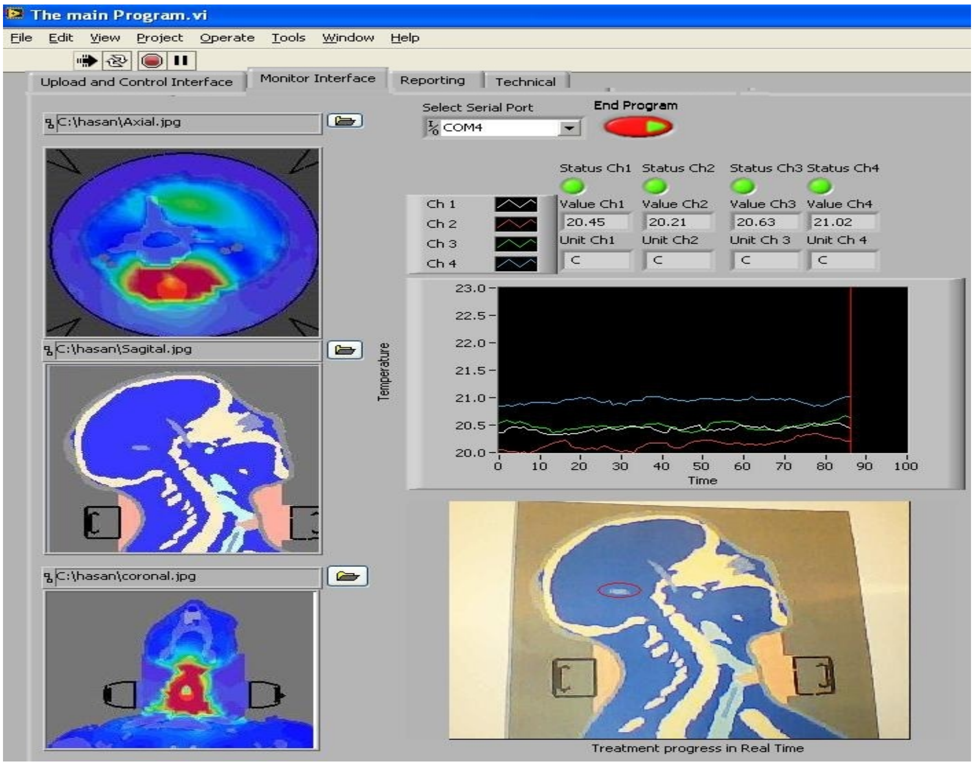

Figure 4.16: The Monitoring Interface.

The reporting tab in figure 4.17 provides with the operator to write about patient details, given treatments and any comments. Once the user change any treatment in the uploading interface and push apply button it will be automatically included in the report. Figure 4.18 shows an example of the report generated from the interface. Here at the beginning patient details and the disease details are included. The time of the report generation is indicated on the top right corner. The form of treatment and time of treatment application is also included to identify the time duration of the treatments. At the end the operator can include his general comments about the treatment procedure and if there any complain from the patient during the treatment. The operator's name will be included in the bottom left corner of the page.

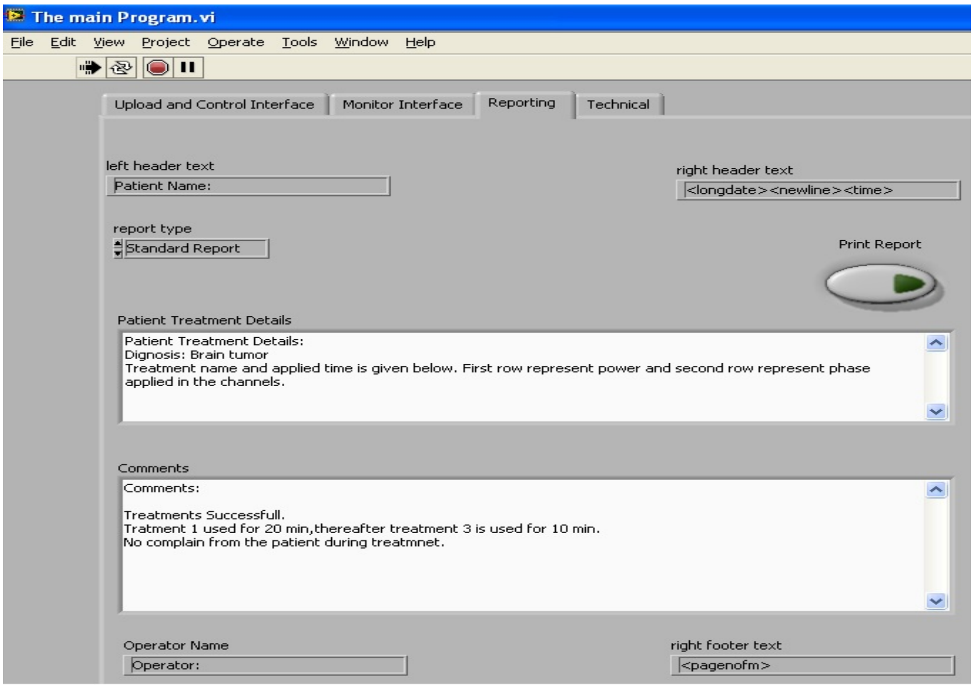

Figure 4.17: The Reporting Interface.

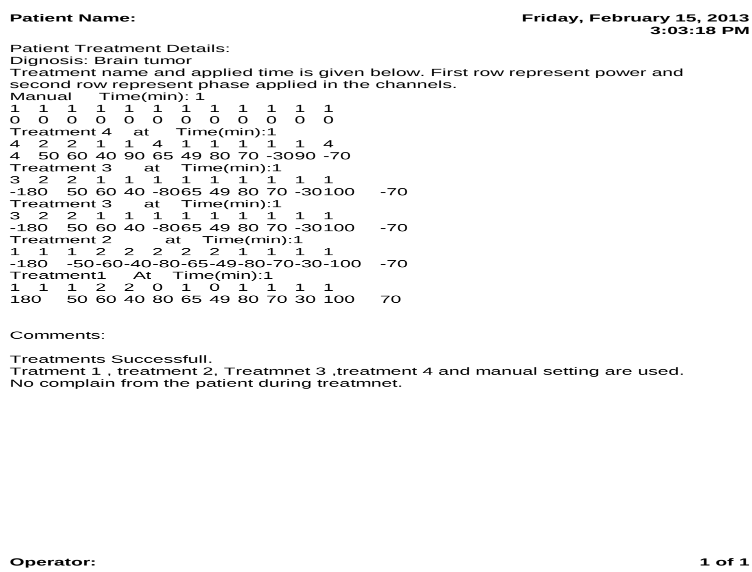

Patient Name: **Friday, February 15, 2013 3:03:18 PM**

Patient Treatment Details:
Dignosis: Brain tumor
Treatment name and applied time is given below. First row represent power and second row represent phase applied in the channels.
Manual Time(min): 1
1 1 1 1 1 1 1 1 1 1 1 1
0 0 0 0 0 0 0 0 0 0 0 0
Treatment 4 at Time(min):1
4 2 2 1 1 4 1 1 1 1 1 4
4 50 60 40 90 65 49 80 70 -3090 -70
Treatment 3 at Time(min):1
3 2 2 1 1 1 1 1 1 1 1 1
-180 50 60 40 -8065 49 80 70 -30100 -70
Treatment 3 at Time(min):1
3 2 2 1 1 1 1 1 1 1 1 1
-180 50 60 40 -8065 49 80 70 -30100 -70
Treatment 2 at Time(min):1
1 1 1 2 2 2 2 2 1 1 1 1
-180 -50-60-40-80-65-49-80-70-30-100 -70
Treatment1 At Time(min):1
1 1 1 2 2 0 1 0 1 1 1 1
180 50 60 40 80 65 49 80 70 30 100 70

Comments:

Treatments Successfull.
Tratment 1 , treatment 2, Treatmnet 3 ,treatment 4 and manual setting are used.
No complain from the patient during treatmnet.

Operator: **1 of 1**

Figure 4.18: The Reporting Document.

The technical tab 4.19 is for technical personnel to diagnose system error and response. The calibration corrections and the reflection information from the channels are included here. If anything is wrong there is chance to stop the treatment directly from here using the stop button.

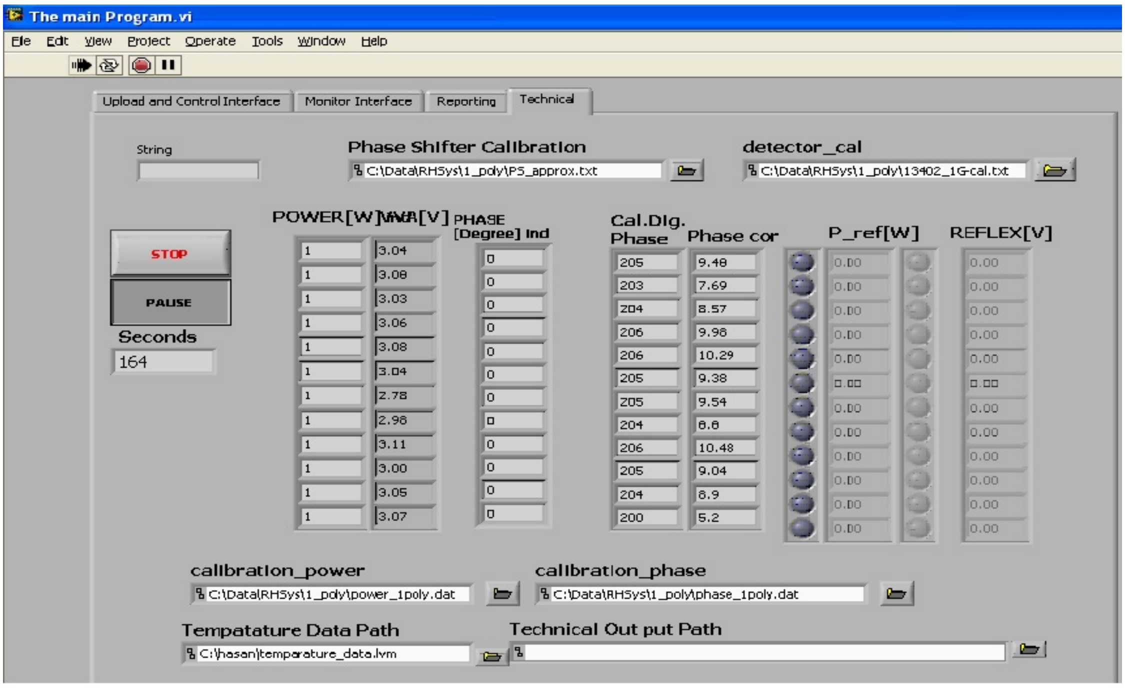

Figure 4.19: The Technical Interface.

4.3 Perfusion Effect

In this section dielectric property of the blood phantom in rest (without any flow) are presented.After this dielectric property during flow change are presented.

In figure 4.20 permittivity of blood phantom at zero perfusion is shown and in the next figure 4.21 the conductivity for the same blood phantom at zero perfusion is also presented.The next two figures shows the dielectric property change in blood phantom dues to the microwaves and different perfusion rates. figure 4.20 shows the permittivity change whereas figure 4.21 shows the conductivity change.

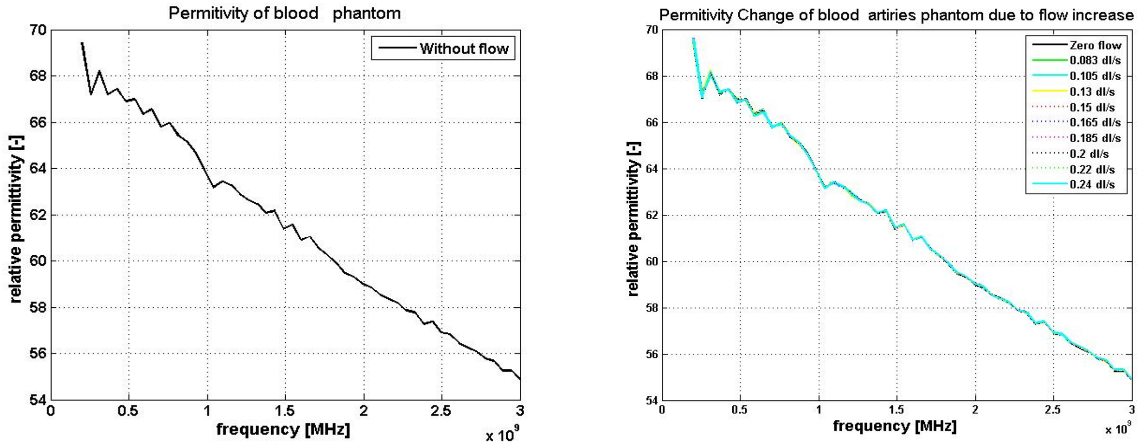

Figure 4.20: Permitivity of blood arteries phantom at zero flow(left) and increased flow(right).

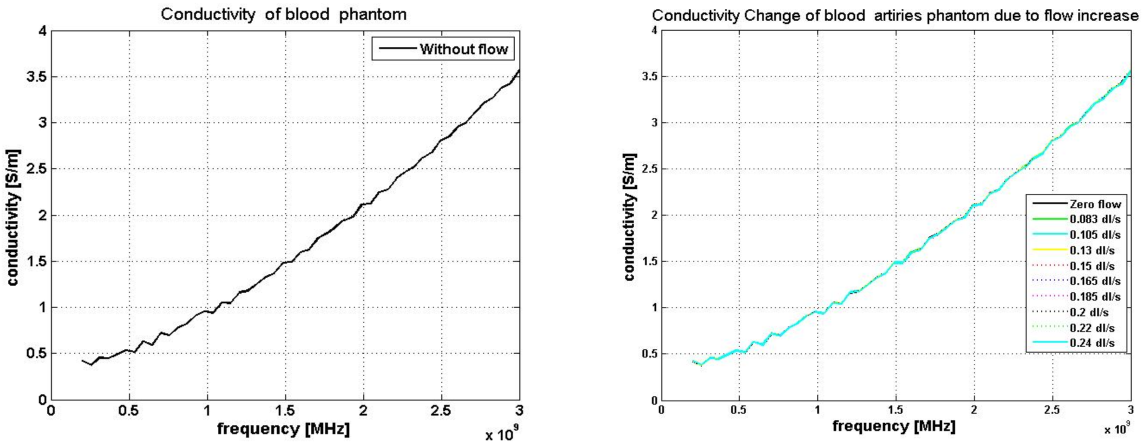

Figure 4.21: Conductivity of blood arteries phantom at zero flow(left) and increased flow(right).

5

Discussion and Conclusion

In this chapter we will discuss about our achievements and the future developments. The first goal of our project was to test the stability of the amplifier system. To test the stability we performed two type of measurements on the hyperthermia system; a long time measurement were carried out for one month duration and a short time measurement lasts for one week duration.

From the long time measurement we found that the system performance is stable up to one month in both phase (maximum 6% error in phase) and power variations (maximum 5.5% error in power) mentioned in long time measurement part of the result chapter and indicated in figure 4.13.

From the short time measurement we found that the worst case phase error is 6% ($14\,^\circ$, at frequency 434 MHz, in ch 05, at allowed phase range $-180\,^\circ$ to $+52.5\,^\circ$) shown in figure 4.3 and the worst case error in the power is 12.5% (-1.25 W) at maximum allowed power shown in figure 4.9.

Thus, the power errors are higher in short time measurements. In the short time measurement the whole system was running for one week without switching off. On the other-hand, while doing long time measurements the measurement to measurement interval was at least one week so the system was not in use for long time. The reason of less time system running is, we performed the long time measurement for one requested frequency whereas in short time measurements five frequencies were used. In the real treatment we would expect to use the system more frequently as short time measurements hereby it is important to find out how it respond during this frequent use.

In figure 4.6, while tracing phase response of channel 09 for frequency 300 MHz at maximum allowed power level (9.8229 W) of short time measurements we found that its' profile is not following the rest of the measurements. Thus less power (9.5 W) than maximum allowed level is used in the new trace shown in yellow line of figure 4.6. It indicates that the new profile matches with others up to a certain phase range and after that it shows the similar behavior as for maximum allowed power. Thus, in order to stay within the allowed phase range, the maximum power level needs to be further restricted.

From the phase variations the short time measurement errors are align with the design criteria but from the power variations, errors are not align with design criteria (error in power accuracy 5% and phase accuracy 5 °)[9][12]. We observed that in frequency below center frequency the full phase range is not covered. Thus, we recommend using 10 bits phase shifter which will allow usage of the full phase range and reducing the phase errors further.

The difference of these two measurements are mainly errors in maximum power and use of long time system running. Thus we recommend, restriction of the maximum power below the saturation level of the amplifiers and avoiding long time system running by switching off the system after each use to resolve short time measurement errors in power and following this the system calibration interval of one month.

In future, for the system to be used in clinics we need to increase the channel power up to 150 W, the system should be placed in an air-conditioned room. To avoid long duration calibration process, implementing an automatic calibration procedure is required. We have to develop a common control platform which will change the amplifier parameters in the hyperthermia system and record the corresponding response from the channels in the VNA.

The second goal was to develop an user friendly graphical interface (GUI) for delivering and controlling the treatment to the patient. The options for uploading treatments, monitor the temperature profile and reporting the treatment were required so that it become more comprehensive to the clinical personnels. We developed a four tabs GUI using Labview programming language which includes Uploading and Control Interface, Monitoring Interface, Reporting interface and Technical Interface.

We have now four sensors supported temperature measurement system but in future we have to increase the number of temperature sensors and provide the facility of viewing temperature profile from these sensors in the monitoring interface. Another graph needed to be included in the monitoring interface which will provide information about temperature mapping into the anatomical features, catheter tracking and margins of radiation. The slice by slice real time treatment needs to be included to compare planned treatment to the treatment in progress.

The reporting has to be improved by including temperature development plot in water bolus. The average and total power applied to the patient needs to be recorded in the report.

The idea of including round shape control of the channels in control interface could not be implemented which would provide further realistic control model because this implementation demands changes in steering codes. Changing the steering codes are not in the scope of this project work.

We recommend the following tasks to be done in future for giving higher usability to the clinical personnel ; including the treatment related plots in the report, direct insertion possibility of patient's treatment information to Patient's Medical Record (PMR) or database and publishing the GUI on the web to allow remote monitoring and control. As interface design is an iterative process there are scope of future development of the interface with the help of user experience.

In a sub-project we investigated the effect of perfusion on the dielectric properties of biological tissues and as results we have found that there is not significant change in permittivity and conductivity of the blood phantom for flow rate of 0.0862 dl/s to 0.24 dl/s. More precise investigation with degassing system is suggested in order to avoid air bubbles inside the blood phantom.

Bibliography

[1] V. Milani, Heat shock proteins, tumor antigenicity and hyperthermia, In Abstract of the 23nd Annular Meeting of the ESHO, Berlin, Germany.

[2] J. G. P Wust, Hyperthermia in combined treatment of cancer, THE LANCET Oncology 3 (2002) Pages 490–495.
URL `http://oncology.thelancet.coml`

[3] H. Trefna, Time reversal near field beamforming for microwave hyperthermiar, Thesis for the degree of Licentiate of Engineering.

[4] H. Trefna, Advances in microwave hyperthermia treatment using time reversal, Thesis for the degree of Doctor of Philosophy.

[5] WHO, Global action against cancer, library catalogue published by world health organization and international union against cancer, Geneva,Switzerland.

[6] Chalmers Microwave hyperthermia, Chalmers University of technology, Sweden, visited 2012,09,01.
URL `http://www.chalmers.se/s2/cha-en/chase/research/microwave-hyperthermia`

[7] E.Cabuy, Hyperthermia in cancer treatment, Reliable Cancer Therapies (2011) Page 4.

[8] D. b. Bhuiyan, Application of hyperthermia for localized drug release from thermosensitive liposomes, Chalmers Library (2010) pages 3–19.

[9] F. J.Bakker, Design and test of a 434 mhz multi-channel amplifier system for targeted hyperthermia applicators, INT. J. HYPERTHERMIA (2010) Pages 158–170.

[10] J. Preece, Y. Rogers, H. Sharp, Interaction design : beyond human- computer interaction, 2002.

[11] H. Trefna, Microwave theremal imaging: towards hyperthermia, Chalmers University of Technology,Sweden (2010) Page 4.

[12] H. Trefna, P. Togni, Design of a wide band multi-channel system for time reversal hyperthermia, Chalmers University of Technology,Sweden (2008) Page 5.

A

Appendix A

A.1 Long Time Measurement Results

In this section all the resutls from long time measurements are presented.

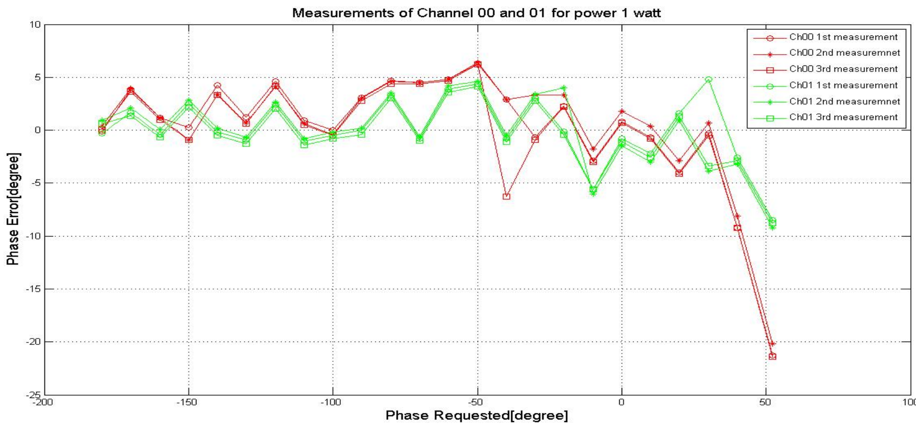

Figure A.1: Measurements of Channel 00 and 01 for Power 1 watts.

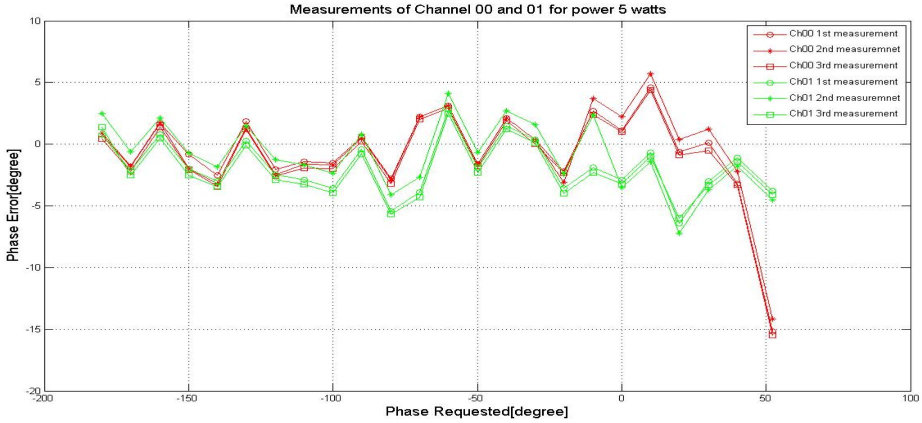

Figure A.2: Measurements of Channel 00 and 01 for Power 5 watts.

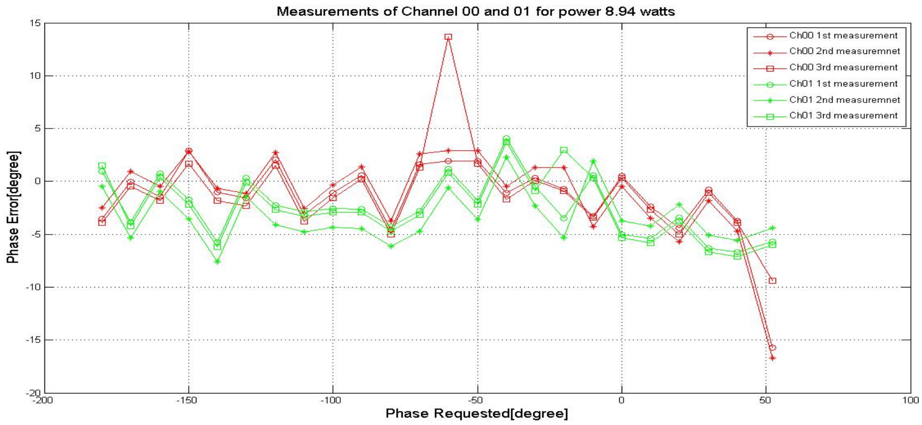

Figure A.3: Measurements of Channel 00 and 01 for Power 8.94 watts.

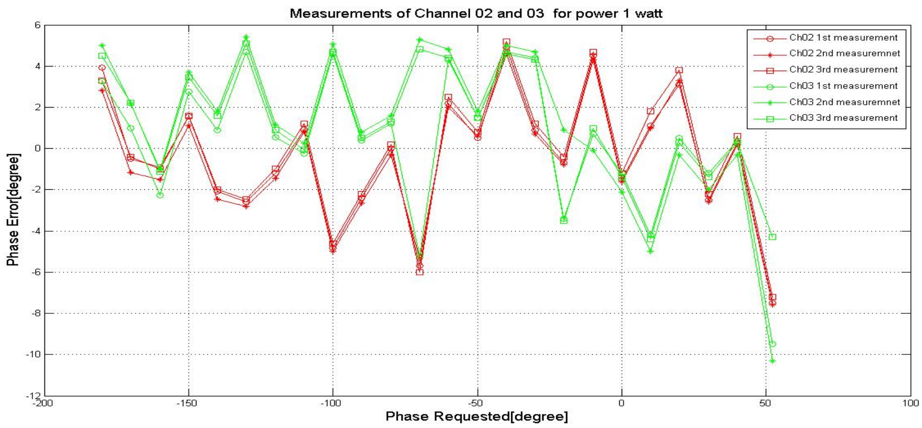

Figure A.4: Measurements of Channel 02 and 03 for Power 1 watts.

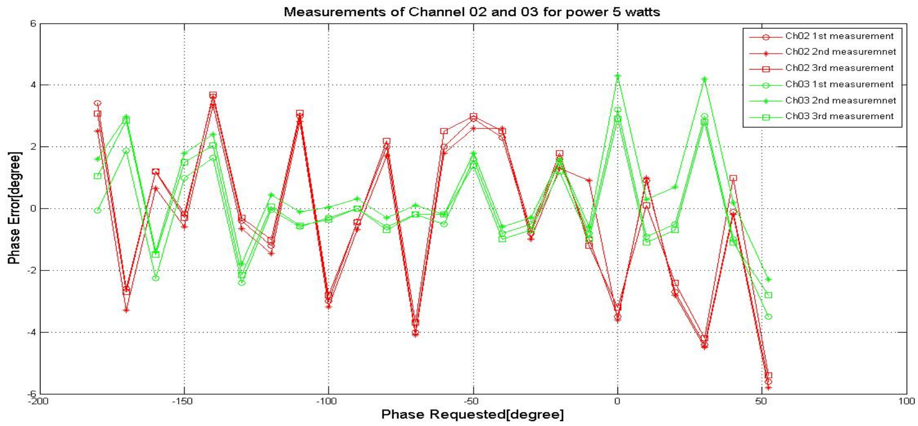

Figure A.5: Measurements of Channel 02 and 03 for Power 5 watts.

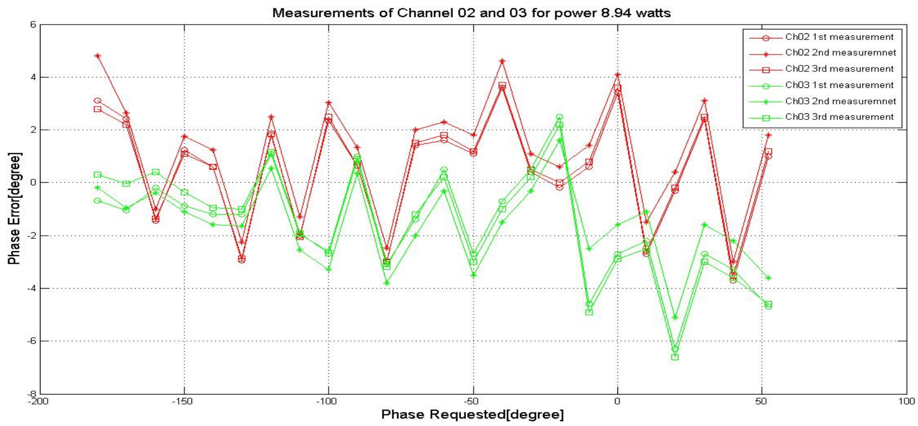

Figure A.6: Measurements of Channel 02 and 03 for Power 8.94 watts.

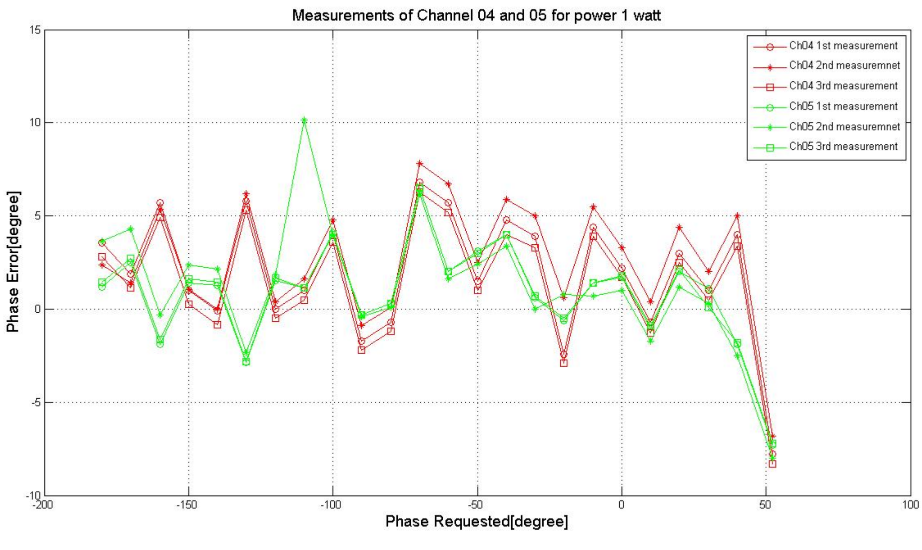

Figure A.7: Measurements of Channel 04 and 05 for Power 1 watts.

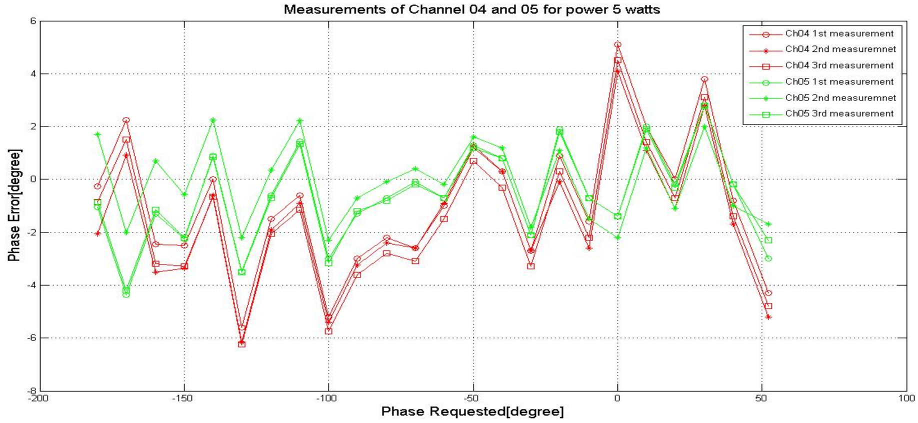

Figure A.8: Measurements of Channel 04 and 05 for Power 5 watts.

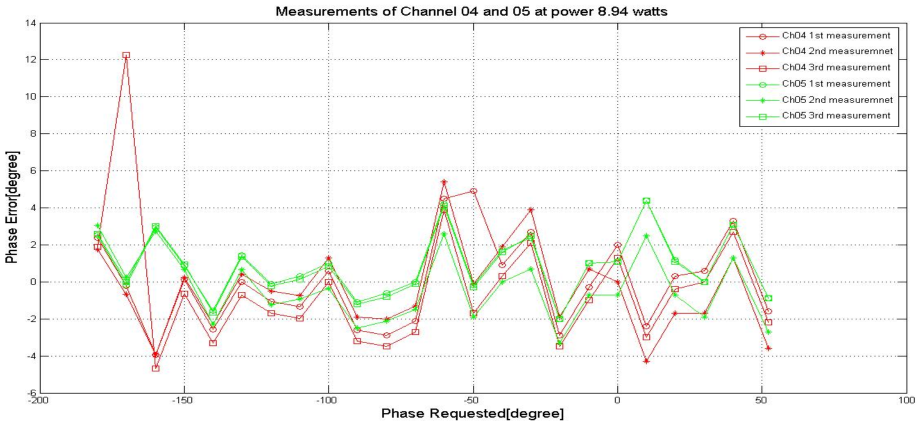

Figure A.9: Measurements of Channel 04 and 05 for Power 8.94 watts.

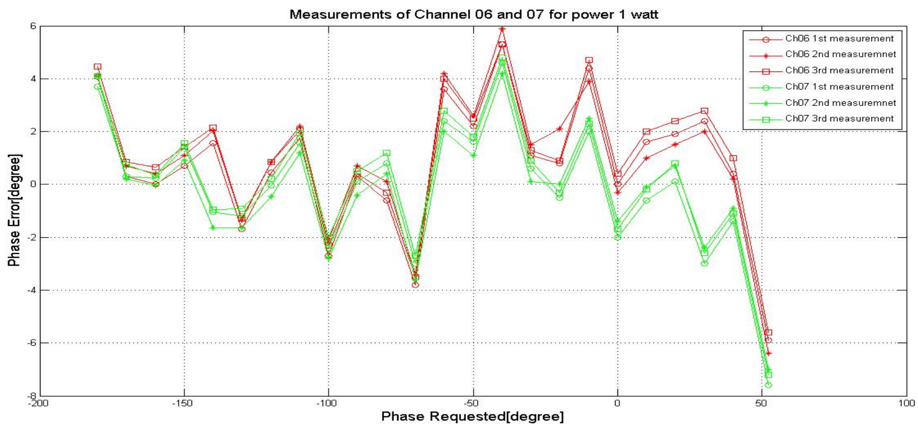

Figure A.10: Measurements of Channel 06 and 07 for Power 1 watts.

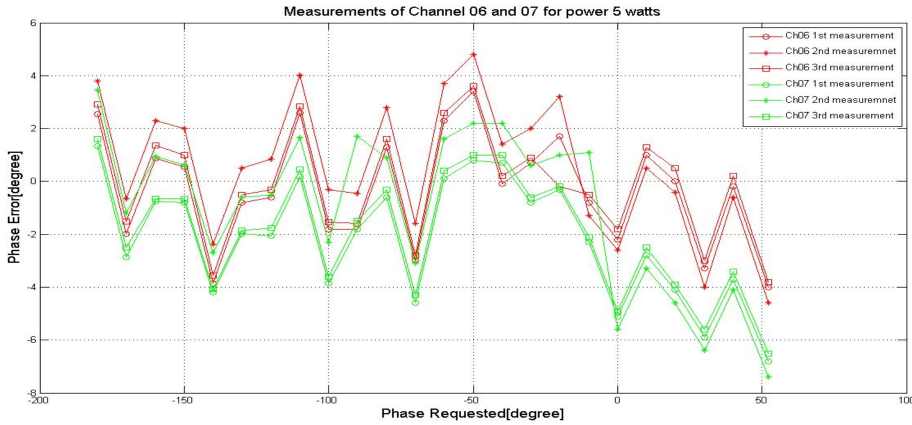

Figure A.11: Measurements of Channel 06 and 07 for Power 5 watts.

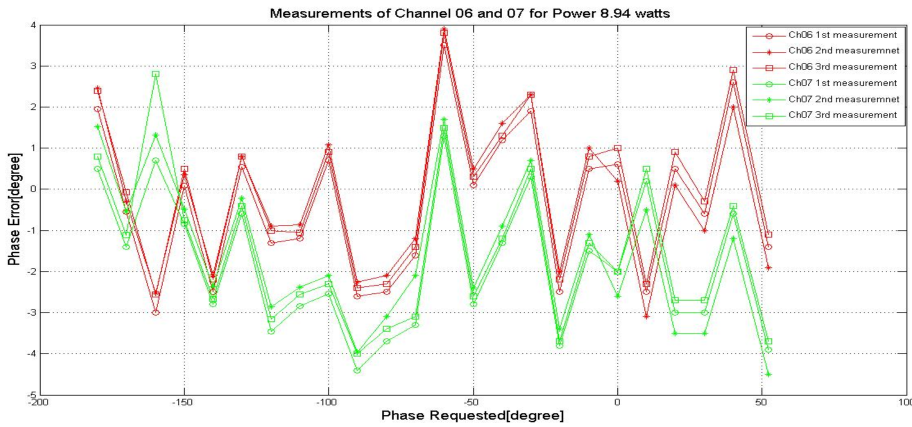

Figure A.12: Measurements of Channel 06 and 07 for Power 8.94 watts.

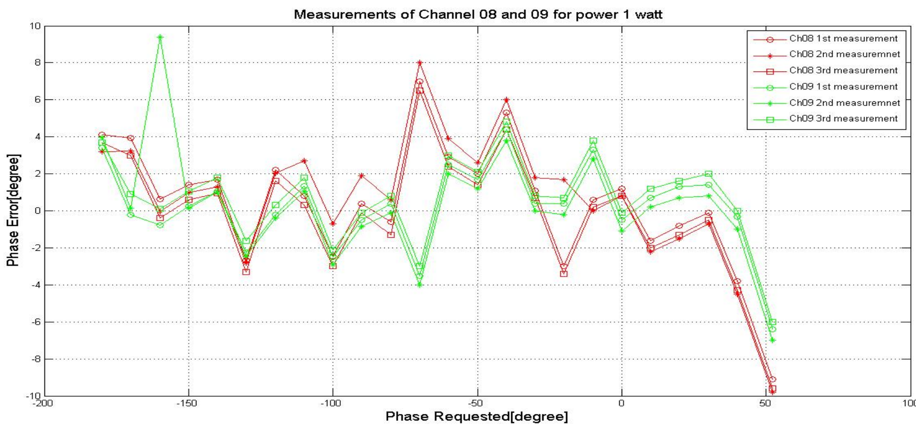

Figure A.13: Measurements of Channel 08 and 09 for Power 1 watts.

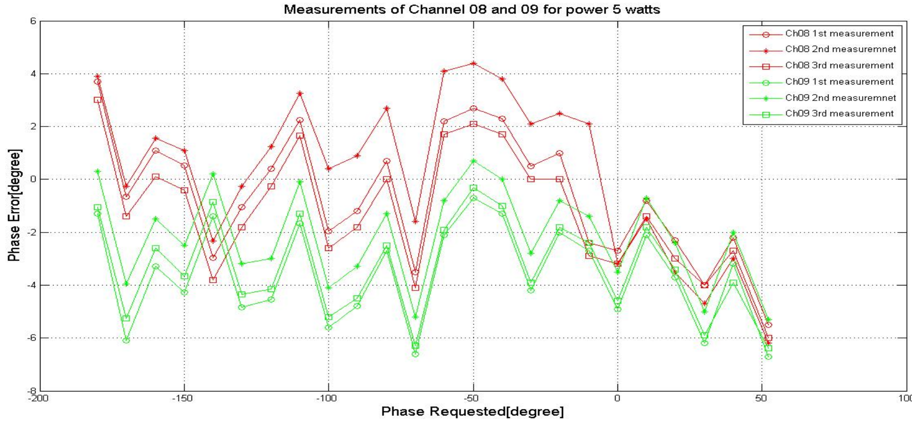

Figure A.14: Measurements of Channel 08 and 09 for Power 5 watts.

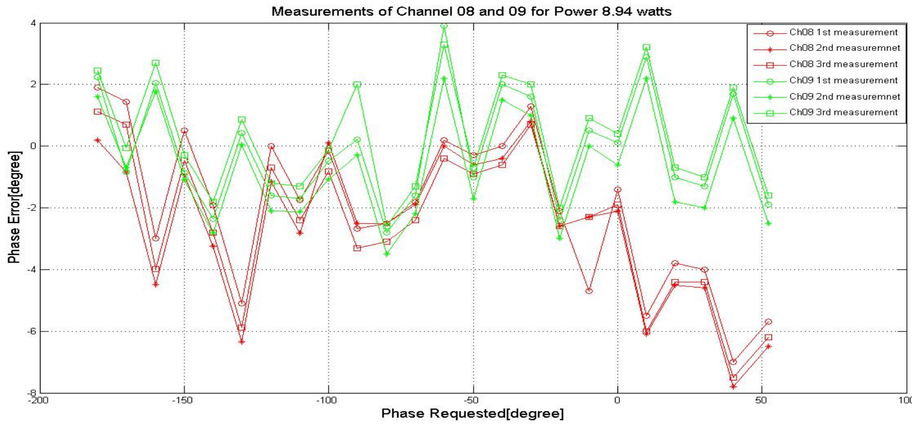

Figure A.15: Measurements of Channel 08 and 09 for Power 8.94 watts.

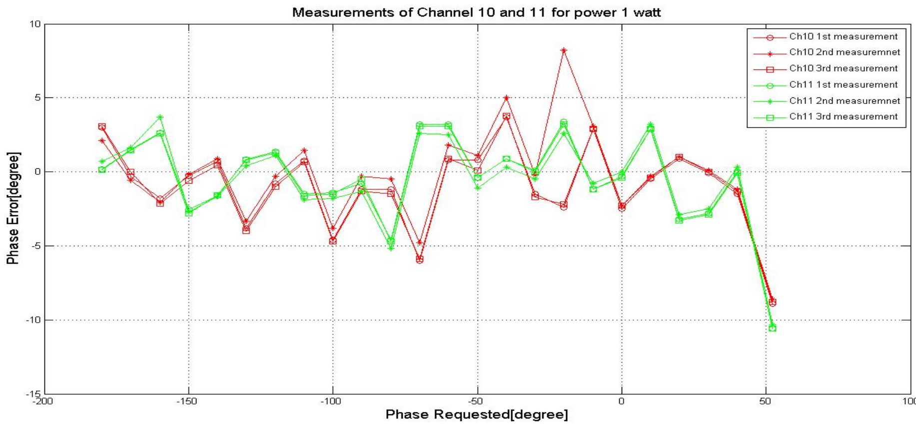

Figure A.16: Measurements of Channel 10 and 11 for Power 1 watts.

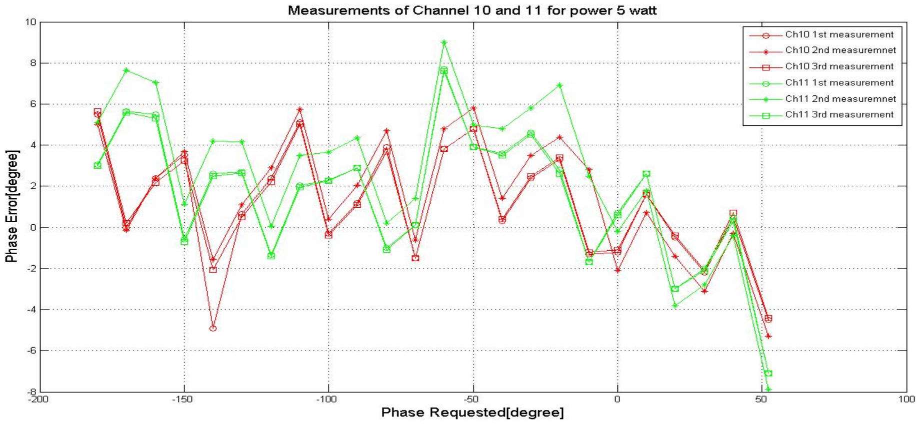

Figure A.17: Measurements of Channel 10 and 11 for Power 5 watts.

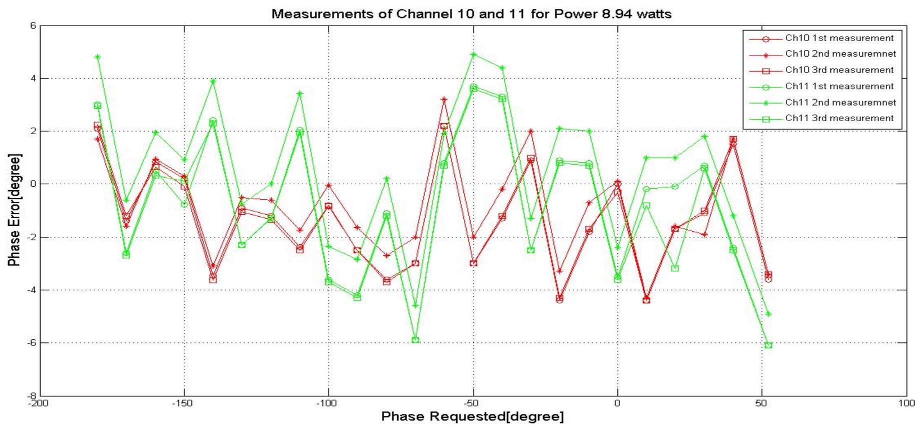

Figure A.18: Measurements of Channel 10 and 11 for Power 8.94 watts.

A.2 Short Time Measurement Results

In this section all the resutls from short time measurements are presented.

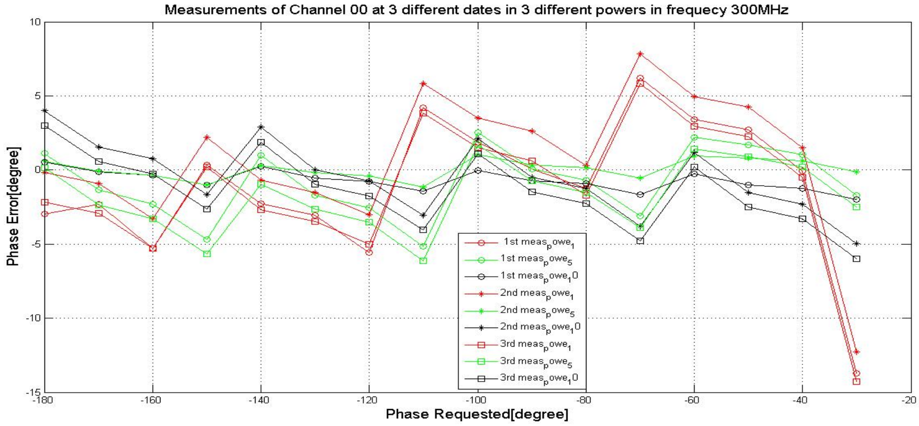

Figure A.19: Measurements of Channel 00 at frequency 300 MHz.

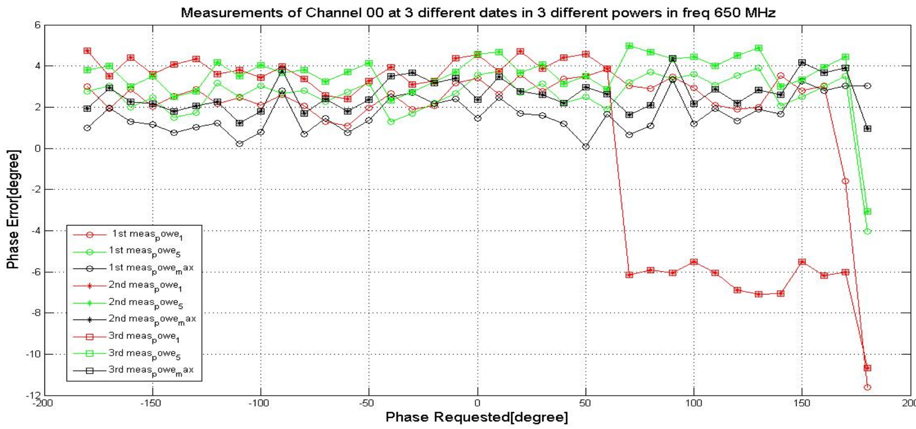

Figure A.20: Measurements of Channel 00 at frequency 650 MHz.

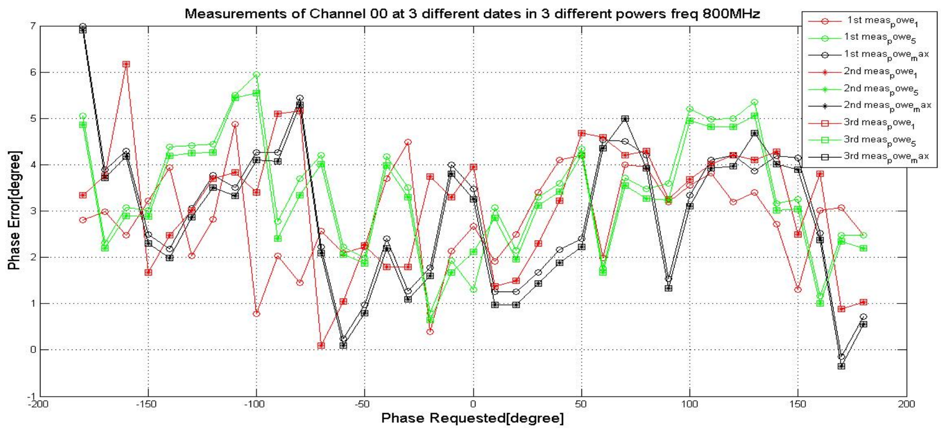

Figure A.21: Measurements of Channel 00 at frequency 800 MHz.

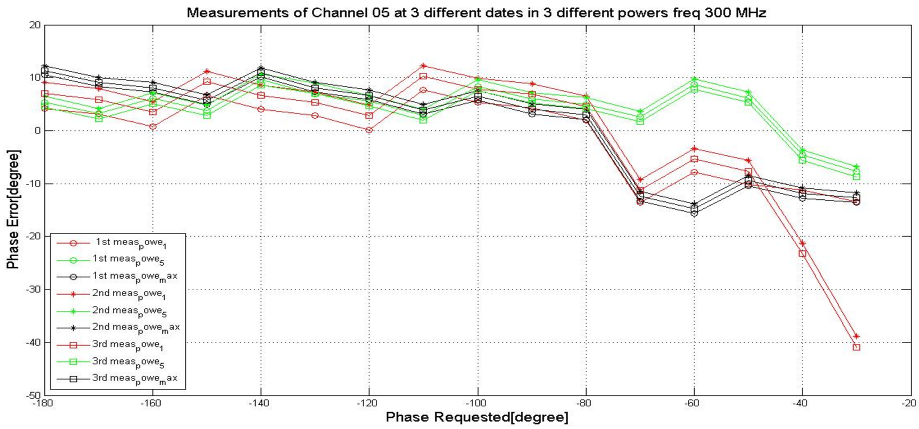

Figure A.22: Measurements of Channel 05 at frequency 300 MHz.

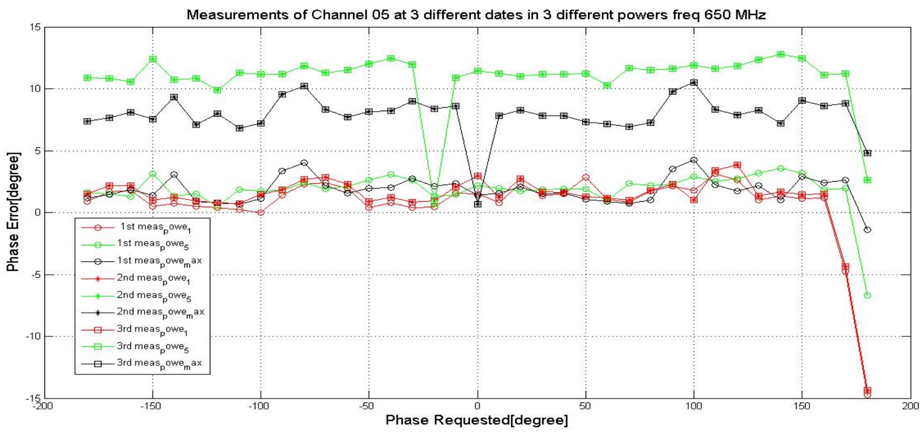

Figure A.23: Measurements of Channel 05 at frequency 650 MHz.

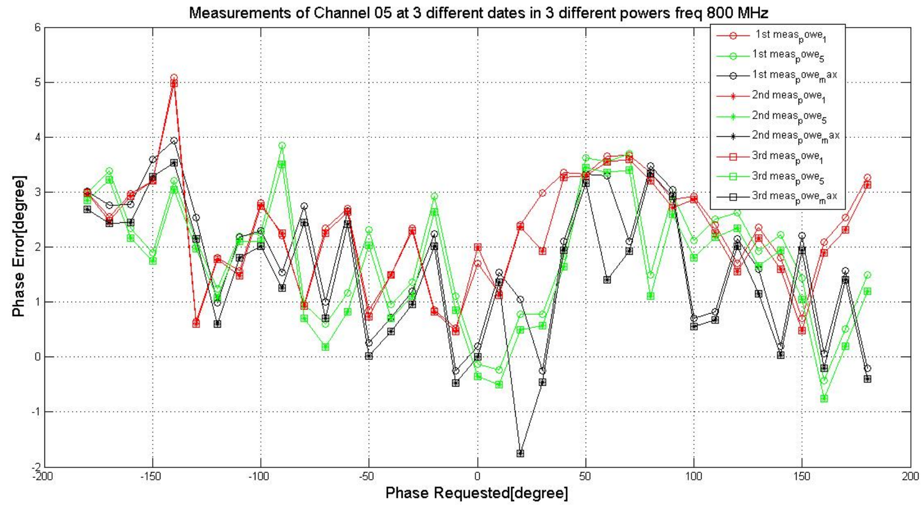

Figure A.24: Measurements of Channel 05 at frequency 800 MHz.

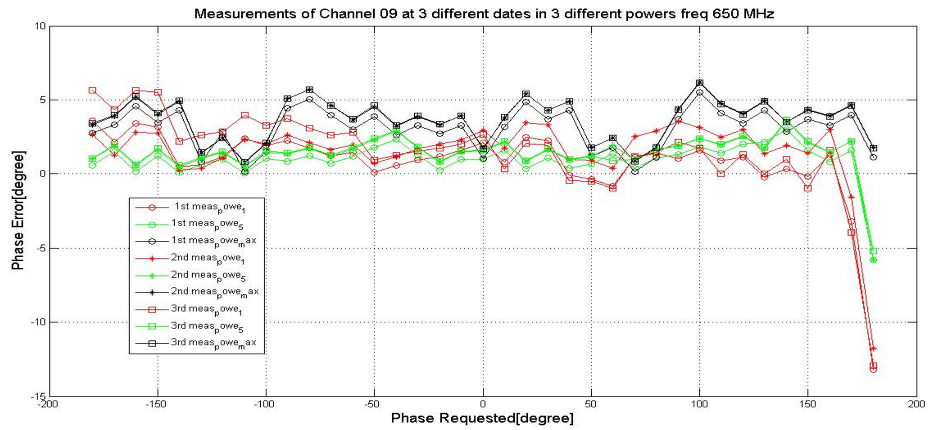

Figure A.25: Measurements of Channel 09 at frequency 650 MHz.

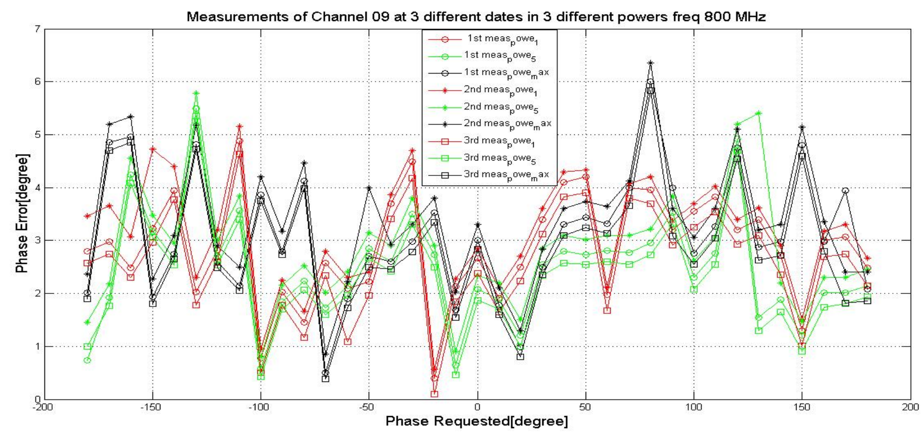

Figure A.26: Measurements of Channel 09 at frequency 800 MHz.

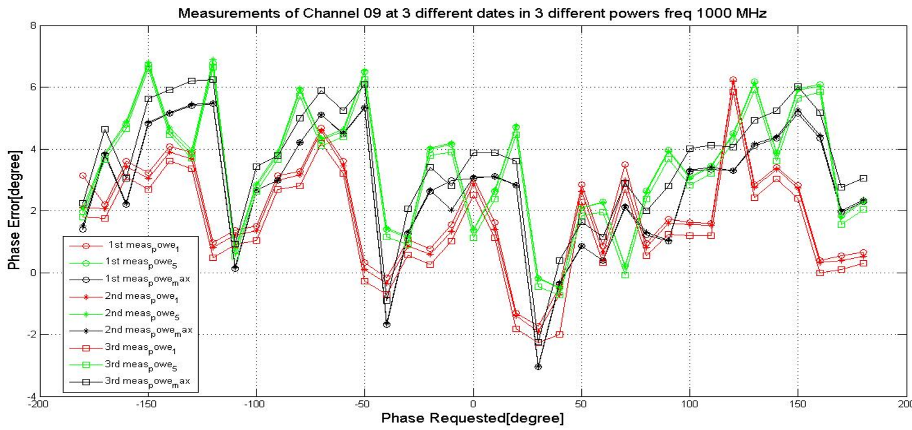

Figure A.27: Measurements of Channel 09 at frequency1000 MHz.